MariaSerena Giliberto

Flow analysis of RANK expression on myeloid cells and identification of bone marrow cells expressing IL-32 in multiple myeloma patients

Master's Thesis

Trondheim, June 2016.

Principle Supervisor: Anne-Marit Sponaas

Co-supervisor: Siv Helen Moen

Norwegian University of Science and Technology

Faculty of Medicine

Department of Cancer Research and Molecular Medicine

NTNU – Trondheim
Norwegian University of
Science and Technology

Acknowledgement

First, I would like to express my deepest gratitude to my supervisor, Anne-Marit Sponaas, PhD for her support and guidance throughout my research. Her continued support led me to the right way. Working with Dr. Sponaas was not just an introduction to the fascinating tool of Flow cytometry but her scientific vision has brightened my path to future success in science. I must acknowledge, Dr. Siv Moen and Professor Therese Standal for their insightful comments and constructive feedback.

Lill Anny and Solveig, no doubt that without you, I would not be able to come this far, so thank you so much for providing me patient's information and bone marrow. I would also like to thank Hanne and Berit for teaching me, every minor detail in cell culture and other experiments.

I cannot forget to mention Marita, Pegah, Zahoor and Menu for their nice company and friendly scientific discussion. It was also fun to have you around and bother you by questions at each step of my experiment. Pegah, being with you, was making everything easy and pleasant in/outside the lab.

My colleague, Neeruja, Demo, Kamila and others, it was a wonderful time that we spent together. Those moments of sharing smile and tears would always be part of my life.

Let me think! How should I express my gratitude to you; it is so difficult, so may be some other time, Mrs. Atla Meås.

Most importantly, none of this would have been possible without the love and patience of my dear parents. It would be my pleasure to dedicate my dissertation to you for being constant source of love, concern, support and strength all these years.

MariaSerena Giliberto

Trondheim, June 2016

Abstract

Multiple myeloma is the second most common hematological cancer worldwide, characterized by an increased expansion of malignant plasma cells in the bone marrow, organ dysfunction, immunodeficiency and bone erosion. Nearly all patients develop osteolytic lesions that cause not only sever bone pain but also promote tumor growth and poor prognosis. Increased osteoclastogenesis is the major cause of myeloma induced bone disease. However, the origin of osteoclast precursors has not yet been fully revealed. One of the prominent markers for osteoclast precursors is RANK expression on their surface, and in this study we determined the expression of RANK in the bone marrow granulocytes and monocytes in myeloma patients.

We determined the RANK expression on granulocytes and monocytes in bone marrow aspirates collected from patients with myeloma by using a multicolor flow cytometric analysis.

Our results showed that very few patients expressed RANK in monocytes and there were significantly fewer $RANK^+$ granulocytes compared to $RANK^+$ monocytes. None of the patients with high tumor load and bone lesions had high proportion of $RANK^+$ granulocytes or monocytes. Based on our results, we are able to conclude that none of these myeloma patients expressed RANK on their granulocytes.

Several pro-inflammatory cytokines are proposed to play an important role in myeloma progression as well as bone disease. Interleukin-32 (IL-32) is a pro-inflammatory cytokine that was found by my research group to be elevated in Multiple myeloma.

In this study we set out to identify the IL-32 expressing cells in the patient's bone marrow in both, $CD138^+$ and $CD138^-$ fractions. Therefore, we performed flow cytometric analysis of patient's bone marrow and myeloma cell lines.

Our flow cytometric analysis showed that IL-32 was highly expressed in two myeloma cell lines whilst very few IL-32 expressing cells could be detected in these myeloma patients's bone marrow. However, a sub-population of $CD138^+$ cells was found to express IL-32. Immunophenotyping of $CD138^-$ fraction suggested that a small proportion of $CD14^+$ monocytes and $CD3^+$ T cells also expressed IL-32.

MariaSerena Giliberto

Table of contents

Abbreviations

ATCC	American type culture collection
BM	Bone marrow
BMECs	Bone marrow endothelial cells
BMM	Bone marrow monocyte
BM-MNCs	Bone marrow mononuclear cells
BMSC	Bone marrow stromal cell
BPT	Bisphosphonates therapy
BSA	Bovine serum albumin
CD	Cluster of differentiation
cDNA	Complementary deoxyribonucleic acid
c-Fms	Colony stimulating factor 1 receptor
CLP	Common lymphoid progenitor
CMP	Common myeloid progenitor
CO_2	Carbon dioxide
DCs	dendritic cells
DKK1	Dickkopf-related protein 1
DNA	Deoxyribonucleotides
ECM	Extra cellular matrix
EDTA	Ethylenediaminetetraacetic acid
ELISA	Enzyme linked immunosorbent assay
ER	Endoplasmic reticulum
FACS	Fluorescence-activated cell sorting
FCS	Fetal calf serum
FMO	Fluorescence minus one
FSC	Forward-scattered light
GAPDH	Glyceraldehyde 3-phosphate dehydrogenase
GMP	granulocyte/macrophage progenitor

HEPES	4-(2-hydroxyethyl)-1-piperazineethanesulfonic acid
HGF	Hepatocyte growth factor
HSCs	Hematopoietic stem cells
IBD	Inflammatory bowel disease
ICAM-1	Intercellular adhesion molecule 1
IFN	Interferon
Ig	immunoglobulin
IL	Interleukin
IMiDs	Immunomodulatory drugs
IMWG	International myeloma working group
MBD	Myeloma bone disease
M-CSF	Macrophage colony-stimulating factor
MGUS	Monoclonal gammopathy of undetermined significance
MIP-1a	Macrophage inflammatory protein
miRNA	Micro RNA
MITF	Microphthalmia-associated transcription factor
MM	Multiple myeloma
MØ	Macrophages
mRNA	Messenger ribonucleic acid
NF-κB	Nuclear factor kappa-light-chain-enhancer of activated B cells
NK	Natural killer
NKs	Natural killer cells
OC	Osteoclast
OPG	Osteoprotegerin
PA	Psoriatic arthritis
PBMC	Peripheral blood mononuclear cell
PBS	Phosphate buffered saline
PCR	Polymerase chain reaction
PCs	Plasma cells

PFA	Paraformaldehyde
PMT	Photomultiplier tubes
PR3	Proteinase 3
Pre-OC	Pre-osteoclast
qPCR	Quantitative PCR
RA	Rheumatoid arthritis
RANK	Receptor Activator of Nuclear Factor κ B
RANKL	Receptor activator of nuclear factor kappa-B ligand
RBC	Red blood cell
SD	Standard deviation
SSC	Side-scattered light
TAC	Tetrameric antibody complexes
TFG-β	Transforming growth factor beta
TNFa	Tumor necrosis factor alpha
TRAP	Tartrate-resistant acid phosphatase
VLA-4	Very Late Antigen-4

List of Figures

List of Table

List of appendices

1 Introduction

1.1 General aspects of Multiple Myeloma

Multiple Myeloma (MM) is a hematological malignancy caused by the accumulation of malignant plasma cells (PCs) in the bone marrow (BM). More than 80% of myeloma patients often suffer from painful bone disease. This leads to severe pain, fractures, vertebral compression and extreme disability [1]. Myeloma patients with bone disease have an increased risk of mortality at least by 20% compared to the patients without skeleton related events [2-4]. Although it is not very well understood, but it is proposed that enhanced osteoclast activity and suppressed osteoblast-mediated bone formation is important for the development of osteolytic lesions. The general hypothesis is that local factors within the bone produced or induced by MM cells, results in either increased bone resorption, or decreased bone formation or both in addition to tumor growth [5].

1.1.1 Epidemiology

Myeloma corresponds to 1.4% of all cancer cases and for 1.9% of all cancer deaths [6]. It is the second most common blood cancer in U.S. with over 20,000 newly diagnosed cases each year. In Norway, 370 new cases of myeloma are diagnosed each year and accounted for 234 myeloma associated death (Cancer register of Norway 2011). Myeloma is most common cancer of the elderly population with a median age of 70 (only 3% of diagnosed patients are under the age of 40) and more prevalent in men than women [6, 7]. Geographically, the frequency of myeloma varies around the world, with the highest incidence in Americans, Canadians and most European countries, whereas lower frequency in Chinese and Japanese population [7, 8]. The incidence rate is higher among African Americans compared with Caucasians [9, 10]. Myeloma, still remains a fatal cancer with an estimated median survival of 3.5-5 [11], although a combination of new (Bortezomib as proteasome inhibitor, or Thalidomide IMiDs) and conventional treatments (chemotherapy) can be beneficial in delaying progression of the tumor. Recently, the median survival time has been extended for the patients diagnosed after 2006 ad treated with new therapy [11].

1.2 Diagnosis and disease progression

Myeloma typically develops through a multistep progression before clinical diagnosis.

Monoclonal gammopathy of unknown significance (MGUS) is recognized as pre- malignant stage of Myeloma, and is characterized by a small number of plasma cells in the BM and low serum level of M-protein [12] but with no clinical manifestations. Well defined criteria have been established by the international myeloma working group (IMWG) to distinguish MM from MGUS and patients with MGUS have an average risk of 1% per year to develop myeloma. The IMWG diagnostic criteria is summarized in table 1.1 [13].

What promotes progression from MGUS to myeloma is not known. One out of the several factors in the development of the neoplastic myeloma cell involves karyotypic instability and acquired genetic changes [14]. Moreover a "permissive" environment for tumor cells has been hypothesized to be the major determinant of such evolution [15].

In MM patients, the malignant cells are clones of the same PCs (monoclonal) and all produce a single type of immunoglobulin or so named M-protein, consisting of heavy chain (most often IgG or IgA, but also IgM, IgD) and a light chain. Of note, in a proportion of cases the malignant cells may produce free light chains (no longer bound to a heavy chain). These free light chains can be quantified in serum, although most light chains are easily excreted in urine.

There are also non-secretory myeloma patients, where the malignant PCs do not produce detectable amount of monoclonal immunoglobulin or free light chains [16]. The most common clinical problems seen in myeloma are due to excessive deposition of misfolded immunoglobulin (Ig) light chains in organs. Such clinical symptoms include hypercalcemia, immunosuppression with increased susceptibility to infections, kidney damage and anemia [17].

Myeloma diagnosis is generally based on identification of increased number of monoclonal PCs in the bone marrow, high level of M protein in serum or urine, and related organ or tissue impairment (ROTI). In clinical practice, the increased number of plasma cells in the bone marrow (>10%) and levels of monoclonal proteins, either in circulation or urine (>30g/L) is considered to indicate progression of MGUS to myeloma [13].

Table 1.1 IMWG diagnostic criteria

Patient Criteria	MGUS	Asymptomatic (SMM)	MM
Serum M-protein	< 30 g/L	> 30 g/L	M-protein in serum and/or urine
Increased BM clonal PCs	< 10%	> 10%	Bone Marrow (clonal) PCs
Related organ or tissue impairment (ROTI)	None	No evidence	Present

MGUS: monoclonal, gammopathy of unknown significance. SMM: smoldering / asymptomatic myeloma. MM: multiple myeloma.

1.3 Healthy and malignant plasma cells

MM is a tumor of terminally differentiated plasma cells. Normal PCs typically reside in the bone marrow as long-live non proliferating cells and are considered the healthy part of myeloma cells [18]. Malignant cells and normal PCs show similarities, as both are long-lived PCs and BM dependent, but they typically display a different phenotype. The phenotype of healthy plasma cells isolated from bone marrow is defined as $CD38^{+}CD138^{+}CD19^{-}CD45^{+}CD56^{-}$ [19]. Malignant plasma cells have commonly positive expression of CD38 and CD138, but as many as 90% of them are $CD19^{-}$, 99% $CD45^{-}$ or $CD45^{low}$, and 70% $CD56^{+}$ [20]. The phenotypic heterogeneity of the clonal malignant plasma cells and its implications are still subject of speculation and most of them are still unknown, but most of these phenotypic differences are largely used to distinguish myeloma cells and healthy PCs [21].

1.4 Genetic events in Multiple myeloma

Substantial research has been conducted into the genetic basis of MM and it reveals a complex genetic nature of this cancer. Translocations, copy number abnormalities, randomly acquired mutations, and miRNA abnormalities are commonly found in myeloma cells. These genetic alterations lead to abnormalities in cell cycle and apoptosis. The *myc* family of oncogenes, acquired Ras mutations (NRAS and KRAS), and IgH translocations at several loci are the most common genetic events involved in tumor progression [22, 23].

1.5 The role of bone marrow environment in myeloma

The tumor microenvironment is considered to be the major player in tumor progression and drug resistance in most cancers including MM. Tumor cells educate their micro-environment and immune

system to turn them from “anti” to “pro” tumorigenic [24]. The presence of myeloma cells in the bone marrow environment is likely to disturb the bone homeostasis leading to bone disease [25].

1.5.1 Components of the bone marrow micro-environment

The spongy bones and the central cavities of the long bones are filled with bone marrow, composed of various cells and non-cellular components, intimately involved in the evolution and propagation of myeloma bone lesions.

The non-cellular component includes a variety of extracellular matrix components ECM proteins (e.g., fibronectin, collagen) which are important to provide support and anchorage for cells; and the soluble components comprises several cytokines, growth factors, and chemokines secreted by hematopoietic and non-hematopoietic cells in the BM [26].

The cellular component consists of hematopoietic and non-hematopoietic cells. Hematopoiesis is a process where hematopoietic stem cell (HSCs) differentiates into hematopoietic progenitors that are further committed to more lineage-restricted precursors: common myeloid progenitor (CMP) and a common lymphoid progenitor (CLP). This occurs within niches in the bone [27].

The hematopoietic cells include stem cells (HSCs), erythrocytes and precursor cells; immune cells such as T lymphocytes, B lymphocytes and plasma cells, natural killer (NK) cells and macrophages (MØ), as well as monocytes, dendritic cells (DCs) and, granulocytes. Moreover, myeloid progenitors give rise to both granulocytes and monocytes.

The non-hematopoietic cells consist of stromal cells, including pericytes, some of which are skeletal stem cells (also known as mesenchymal stem cells), bone marrow adipocytes, fibroblasts, bone marrow endothelial cells BMECs, as well as osteoclast and osteoblasts. In addition, osteocytes are embedded in the bone matrix and are usually described as terminally differentiated osteoblasts [28].

Communication between MM cells and the bone marrow cells is achieved by direct cell-cell contacts and indirect release of cytokines within the extracellular matrix [29, 30]. The end result of these interactions between neighboring cells such BM stromal cells (BMSCs) and other immune cells (e.g. T cells and monocytes) [31], is the release of several paracrine signals, which in turn act as survival factors of the myeloma cells as well as induce the production of pro-osteoclastogenic factors, that promote the development of bone disease [32]. Adhesion of tumor cells to local BM tissue is mediated through several adhesion molecules expressed by both tumor and stromal cells [33]. For instance, very late antigen 4 (VLA-4), intercellular adhesion molecule 1 (ICAM-1, CD54), and syndecan-1 (CD138) mediate binding of myeloma cells to both ECM and BMSCs [34]. Cell surface syndean-1 has been shown to drive tumor growth as well bone resorption [35, 36].

1.6 Myeloma induced Bone Disease

Bone is a dynamic organ where remodeling takes place throughout the life span of an individual. Under healthy conditions, the bone turn-over is tightly regulated, consisting of old bone resorption by osteoclasts and synthesis of new bone tissue by osteoblasts [37]. As previously mentioned, Myeloma bone disease (MBD) develops as a consequence of multiple interactions between myeloma cells and other cells in the BM environment. In addition to disturbed immune cell functions (for example T cells, monocytes), bone cells like osteoblasts and osteoclasts show significant impairment in myeloma bone disease [38, 39].

The bone impairment is not confined to MM only, but is also associated with several other cancers and inflammatory diseases including rheumatoid arthritis (RA) and psoriatic arthritis (PA). However, MM is unique in this context as there is no new bone synthesis as well as increased bone resorption. In breast and prostate cancers , on the other hand, both osteoclast and osteoblast activity are increased [37]. The bone lesions in myeloma , can be either in the form of localized lesions, or multiple lytic lesions affecting any part of the skeleton (generalized osteoporosis) [37]. This suggests that both local and systemic factors are equally implicated in the development of myeloma bone disease [40]. Histological studies of bone biopsies from myeloma patients showed that myeloma cells were found close to the site of active resorption, suggesting that the bone loss is mediated by direct cell-contact [4].

Several osteoclastogenic factors are up regulated in the myeloma bone marrow, following myeloma cells adhesion to the bone matrix. In particular, receptor activator of NF-kB ligand (RANKL) [41], macrophage-colony stimulating factors (M-CSF), macrophage inflammatory protein-1 (MIP-1a), transforming growth factor beta (TGF-β), hepatocyte growth factors (HGF), vascular endothelial growth factor (VEGF) as well as several inflammatory cytokines IL-1β, IL-3, and IL-6, produced by both myeloma cells as well as BMSCs [28]. An inflammatory state within myeloma environment is likely to enhance the sensitivity of osteoclast precursors to ligands such as (RANKL) as well as to additional mitogenic factors, thereby accelerating osteoclast maturation. Conversely, osteoblast suppression and decreased bone formation are due to dysregulation [42] of several signaling molecules such as DKK1 [43], IL-3 and IL-7 [44]. The activated osteoclasts also provide feedback signals to the myeloma cells facilitating their proliferation and survival. This is often referred to as the "vicious cycle" [30] (Figure 1.1) of myeloma-osteoclast interactions [45, 46]. In fact, it was found that osteoclasts help tumor propagation by releasing a number of angiogenic factors (including IL-6, IL-1b, TNF-a and osteopontin OPN) that in concert with other BM factors, induce increased survival of myeloma cells [32], clearly highlighting the key role that bone disease plays in MM [46].

Myeloma patients with bone disease require treatment with biphoshonate (BPT) as well as analgesic drugs in addition to the standard anti-myeloma therapy (Bortezomib), immunomodulatory drugs (IMiD) Thalidomide and chemotherapy [47]. Some patients may additionally need radiotherapy and

surgical interventions. However, as BPT therapy only reduces skeletal-related events by 50% and new therapies to treat MM related bone disease are needed [48].

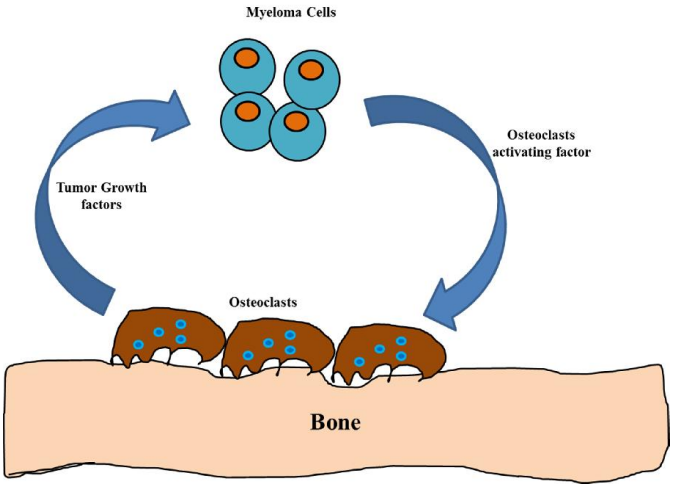

Figure 1.1 Illustration of the "vicious cycle" of bone erosion and tumor growth.

Myeloma cells secrete or induced soluble factors involved in MM-induced osteoclasts activity. Osteoclast induced bone resorption releases growth factors embedded in the bone matrix that increases tumor growth. *The figure is drawn by the author.

1.7 Osteoclast and the role of RANK in osteoclast development

1.7.1 Osteoclast: bone resorbing cells

Osteoclasts are derived from common myeloid progenitors (CMPs) of the monocyte-macrophage lineage. They differentiate through sequential stages to non-dividing, multinucleated bone resorbing cells. Early osteoclast precursors (OCPs) are seen in both granulocyte-macrophage progenitors and mature monocyte subsets (Figure 1.2) [49]. On note, some studies suggest the existence of a common axis from, granulocyte/macrophage progenitors (GMPs), which can give rise to mature granulocytes, macrophages (MØ), osteoclasts and early dendritic cells (DCs) [50]. At the end of their differentiation, osteoclasts adhere to the bone surface and release acids and bone-degrading enzymes such as tartrate-resistant acid phospahatase (TRAPc), cathepsin K, and metalloproteinases resulting in the breakdown of bone [32]. The regulation of osteoclast fate is strongly dependent on cytokine exposure (e. g. TNF-a, IL-3), expression of transcription factors PU.1 and microphthalmia (MITF) as well as additional signaling mediated by c-Fos the receptor for macrophage-colony stimulating factor (M-CSF) and the ligand of the TNF superfamily member RANKL [51].

1.7.2 RANK in osteoclast development

In normal and pathological conditions such as inflammatory diseases or cancer, bone remodeling is regulated by Receptor Activator of Nuclear Factor kappa B, RANK (also known as TNFRSF11A, TRANCE) and its ligand RANKL as well as by soluble decoy Receptor Osteoprotegrin (OPG). RANK is a trans-membrane receptor and belongs to TNF receptor superfamily of proteins [52, 53]. Ligation of RANK to its ligand RANKL, which is expressed and secreted by stromal cells as well osteoblasts, induces fusion and maturation of osteoclast progenitors resulting in the formation of multinucleated OCs. However, the presence of macrophage-colony-stimulating-factors (M-CSF) on early stage of osteoclast precursors is essential to provide signals for survival and proliferation by its receptor c-Fms and up-regulation of RANK [54, 55] (Figure 1.2). OPG is a decoy receptor to RANKL. The Rank signaling pathway is negatively controlled by osteoprotegrin (OPG) by inhibiting the binding of RANKL to its receptor RANK [56]. OPG (TNFRSF11B) belongs to the TNF receptor family and is produced by various cells including osteoblast. Overexpression of OPG was found to antagonize OC formation and induces osteopetrosis in transgenic mice, lacking *csf1r*, gene coding for the M-CSF [52, 57, 58].

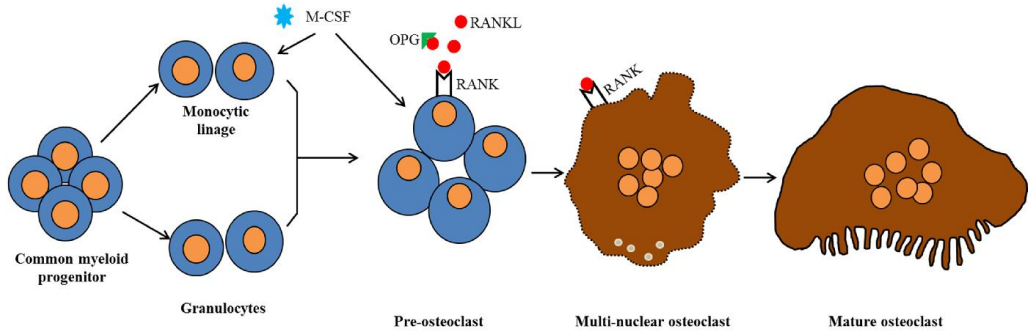

Figure 1.2 Figure illustrates osteoclast differentiation from precursor cells into mature osteoclasts in the bone. Progenitors are fused to form multinucleated and mature osteoclasts. *The figure is drawn by the author.

1.8 RANK expression on osteoclast precursors

Although osteoclasts are the most important cells in pathological conditions characterized by increased bone erosion, their cellular origin is not fully identified and their differentiation pattern is not clearly understood. It is suggested in the literature that RANK is an important barcode for pre osteoclast identification. $RANK^+$ monocytes are found in the periphery as well as in the bone marrow. Only a minor fraction (1-2%) of the $CD14^+$ monocyte subsets in peripheral blood can differentiate into osteoclasts [59]. However, RANK expression is not only confined to monocytes, as RANK was detected on other cell types in peripheral blood and bone marrow mononuclear fraction in addition to monocytes [60]. This study reported that a minor population of $CD34^+$ hematopoietic progenitors and $CD3^+$ T cells was found also to express RANK. In addition RANK was present on $CD19^+$ B cells as

well as on $CD56^+$ Natural killer cells (NKs). Adding further, immature murine dendritic cells could also differentiate into functional osteoclasts in vitro and vivo in the bone marrow environment in the presence of activated T cells [61]. In the case of MM it was recently showed that immature dendritic cells have the ability to differentiate into osteoclasts after IL-17A stimulation [62].

1.9 IL-32: a potential role in Myeloma bone disease

Although, several factors play important roles in the myeloma-induced bone erosion, many of the underlying mechanisms are not understood. In our group, it was recently found that interleukin 32 (IL-32) is one of the genes highly expressed in primary myeloma cells from patients. IL-32, is a novel pro-inflammatory cytokine, formerly known as NK4 (Natural Killer cell transcript 4) was identified as a gene highly expressed in immune cells like Natural killer cells (NKs) and T cells upon activation and act primarily on monocytic cells [63]. Later on it was, identified as a pro-inflammatory cytokine that induces the expression of TNF-α, IL1β, IL8 and IL6 [64, 65]. It was found to differentiate human blood monocytes in to macrophages and enhanced their phagocytic activity against bacteria [66]. In addition, Kim and collogues (2008) reported that IL-32 is a key promoter of osteoclast differentiation from human $CD14^+$ monocytes in vitro. It was proposed that IL-32 synergized with RANKL and enhanced the fusion of pre-osteoclasts, resulting in the formation of multi-nucleated osteoclasts [67] or alternatively promoted interactions between RANKL and RANK on osteoclast precursors. IL-32 was found to be highly expressed in synovial tissues of patients with RA and to be involved in the disease progression of (RA) [68]. Moreover, IL-32 has been considered to be important in innate host defense, including mycobacterial or viral infection and to play a key role in cancer development and metastasis [69-72]. For example, leukemia cells that were resistant to TNF-alpha induced cell death became sensitive when co-cultured with bone marrow stromal cells that expressed high levels of IL-32. This was inverted when IL-32 expression was inactivated [73]. Several authors have proposed a mechanism by which proteinase-3 PR3, binds or cleaves IL-32 and resulting in an increased activity of IL-32 on the cell membrane. Active IL-32 activates several signaling pathways to induce the expression of different cytokines and promote cellular growth and survival [74, 75]. However, it is not known whether it is expressed in multiple myeloma.

2 Aims and objectives of the project

The study of RANK expression in myeloma patient's bone marrow

Myeloid cells such as monocytes, granulocytes as well as osteoclast precursors share a common progenitor as well as effector functions such as phagocytosis**.** Recently reports shows an increased expression of RANK in a population of granulocyte subsets from patients with bacterial infections and patients with RA compared with healthy donors. It was also found that these cells could differentiate into osteoclasts in vitro [76]. This raised an important question, whether granulocytes from myeloma patients express more RANK and that this may increase the pool of pre-OC like cells prone to undergo osteoclast differentiation.

IL-32 expression in myeloma patient's bone marrow

As it suggested that IL-32 has diverse roles in various cell types, we became interested to check the expression of IL-32 in multiple myeloma. Considering the heterogeneity of myeloma cells, identifying an IL-32 expressing malignant cell population would also add additional information in the understanding the role of IL-32 in myeloma pathogenesis. We also wanted to identify which cells other than malignant plasma cells are expressing IL-32 in the bone marrow of myeloma patients.

The aims of these studies are:

- To identify whether a population of granulocytes in the bone marrow from myeloma patients expresses RANK. Monocytes, as an established source of osteoclast precursors were evaluated for RANK expression in the same bone marrow samples as well.
- To assess the presence of intra-cellular IL-32 in the bone marrow of myeloma patients

The objectives of these studies are:

- Examine the RANK expression on monocytes and granulocytes in unseparated bone marrow aspirates of myeloma patients, using a multi-color flow cytometric assay.
- Asses the presence of intra-cellular IL-32 in myeloma cell lines, in order to establish a protocol by flow cytometry.
- Investigate IL-32 expression in primary myeloma cells ($CD138^+$), ($CD138^-$) from patient's myeloma bone marrow mononuclear fraction by flow cytometry.
- Investigate IL-32 expression on distinct cells types T cells, B cells and monocytes by 4-color flow cytometric assay

3 Materials and Methods

3.1 Patient samples

Samples used in this study comprised bone marrow aspirates taken from multiple myeloma patients.

3.1.1 Unseparated bone marrow biopsy

Bone marrow aspirates were collected from patients registered in the Norwegian Myeloma Biobank and enrolled in the study (Biological mapping of Multiple Myeloma). The study was approved by the Regional Ethics Committee (REK 2011-2029). Normally, 20 ml bone marrow aspirates were collected from the Iliac Crest of the patients in Na-Heparin containing tubes to avoid clotting. Only freshly isolated bone marrow samples were subjected to flow cytometric analysis. Donors were classified as MGUS and multiple myeloma according to the international myeloma working group criteria [13]. Bone marrow PC percentage was routinely performed by May-Grunwald-Giemsa stained smears. Clinical data for patients used in the RANK study are shown in the Table 1, however the patients information in IL-32 studies were not yet available.

Table 3.1 Clinical/laboratory data at diagnosis in multiple myeloma patients

Patient ID	Sex	Age	%PC (Smear)	M COMP. g/L	Subtype	Treatment	Diagnosis	Osteolytic Lesions
1540	F	70	X	X	X	X	x	x
1542	M	73	X	24	IgG k	Untreated	Myeloma	x
1544	M	63	2	8		Untreated	Myeloma	Yes
1421	F	76	X	X	X	X	x	X
302	F	86	30-40	29	IgG k	Treated Earlier	Myeloma Relapse	Yes
1494	M	79	38	8	IgA k	Untreated	Myeloma	X
1500	F	67	65	X	IgG k	Treated	Myeloma	Yes
1502	M	77	2	1/3,5	IgA/IgM	Untreated	MGUS?	No
1519	M	68	X	X	X	X	X	X
1539	F	58	95	62	IgA k	Untreated	Myeloma Relapse	Yes
1334	F	53	70		free lambda	Untreated	Myeloma	Yes
1348	x	x	x	x	x	x	No Myeloma	x
1349	M	66	21	36.3	IgA k	Untreated	Myeloma	x
1490	x	x	x	x	x	x	x	x

x data not available

3.2 Separated bone marrow biopsy

3.2.1 Bone marrow mononuclear cells (BM-MNCs)*

Bone marrow mononuclear cells (BM-MNCs) were isolated by density gradient separation procedure. The entire separation procedure was performed in BD Vacutainer® Cell Preparation Tube™ (hereafter named CPT) containing a citrate anti-coagulant with the cell separation medium (Ficoll Hypaque 400), which is composed of a gradient fluid and a polyester gel (BD Biosciences information website).

The collected sample is diluted with an equal volume of a Ca^{++}/Mg^{++} free Phosphate Buffered Saline (PBS) and layered on cell separation medium. The CPT is then centrifuged at 1800 g for 30 minutes at room temperature (20-25 ^{o}C) to separate different cellular fraction based on density. The BM-MNCs will form a distinct chalky layer with other cells of same density (e. g. platelets) in the middle between plasma and density medium due to their relatively low density. While other high density cells, including granulocytes and red blood cells will gravitate toward the bottom of the tube as a two separated layers (Figure 3.1). The BM-MNCs layer is carefully pipetted out and collected in a 15 mL conical tube followed by washing twice at 300 g for 10 minutes at room temperature to remove platelets.

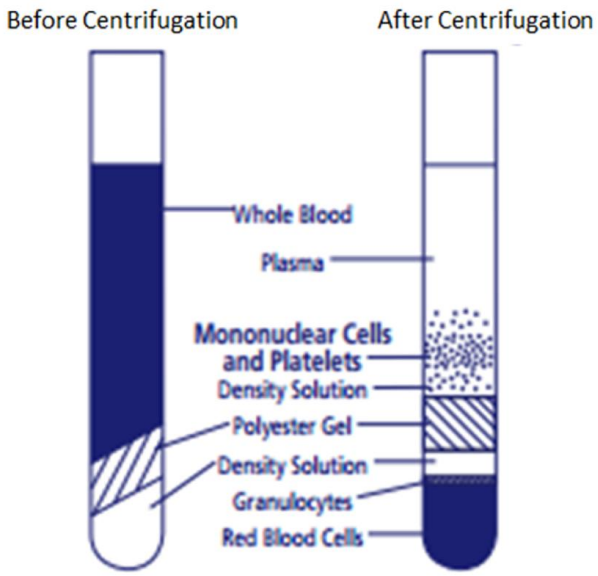

Figure 3.1 Illustration of BD Vacutainer® Cell Preparation Tube™ and BM-MNCs isolation procedure.
The image is adopted from BD vacutainer® CPT datasheet.

---

* The isolation procedure was performed by the Norwegian Myeloma Biobank laboratory

3.2.2 CD138^{+} cells isolation procedure

Subsequently, CD138^{+} plasma cells enrichment was achieved by using EasySep-Human-CD138 Positive- selection kit in combination with EasySep Magnetic beads and automated cell separator RoboSep (StemCell Technologies, Grenoble, France). The isolation is based on the principle of antibodies specify and magnetism.

The positive selection cocktail contains a combination of monoclonal antibodies designed to provide pure cell population of CD138^{+} cells. The CD138 antigen (Syndecan 1) is primarily found on normal as well as in most MM plasma cells in the bone marrow (but not on mature B cells), and is therefore, used as a common myeloma cell specific antigen [77, 78]. Desired cells were allowed to bind with dextran-coated magnetic beads using Tetrameric Antibody Complexes (TAC). The TAC is a complex in which antibodies at one end recognizes dextran (the magnetic beads are dextran coated) and antibodies on other side are designed against CD138^{+}, while both are connected via linker (Figure 3.2). This cocktail also contains antibodies against human Fc receptors to minimize nonspecific binding. The cells were collected in a 14 mL polystyrene tube to properly fit into the RoboSep magnet. Positive selection cocktail was added to the single cell suspension and incubate for 15 minutes at room temperature. The cells were further incubated with magnetic particles for 10 minutes at room temperature. Then, the mixture containing cells along with antibodies cocktail and magnetic beads are placed next to a RoboSep magnet. Positively selected CD138^{+} cells were magnetically retained in the tube, whereas the supernatant fraction was poured off as negative fraction (CD138^{-}), compromising T cells, B cells, monocytes and others (Figure 3.2). The purity of CD138^{+} plasma cells is reported to be above 90% and similar purities were obtained in our lab.

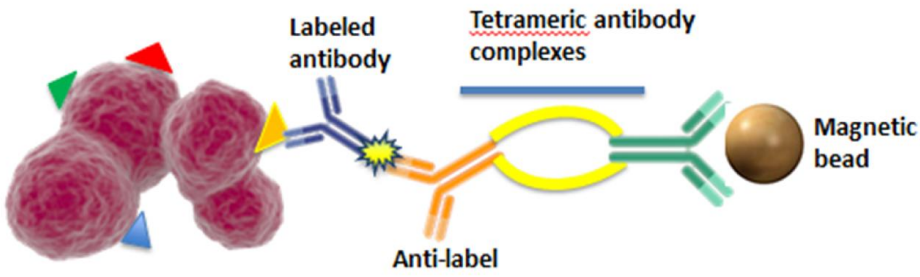

Figure 3.2 Schematic presentation showing the mechanism of EasySep® Tac Magnetic Human cell labeling.

Tetrameric Antibody Complexes of two mouse IgG1 monoclonal antibody forming a tetrameric structure. The structure is held together by two rat anti-mouse IgG1 monoclonal antibodies. One mouse antibody recognizes membrane antigen CD138, the other one is against dextran on the magnetic particles. EasySep Magnetic nanoparticles do not interfere with subsequent flow cytometric analysis. * The figure is drawn by the author.

3.3 Cells and Cell culture

Three human myeloma cell lines JJN-3 (a kind gift from Dr. J. Ball, University of Birmingham, UK), H929 (purchased from American Type Culture Collection (ATCC), Manassas, VA, USA), and CAG (a kind gift from Professor Leif P. Bergsagel, Little Rock, AR) were culture in RPMI-1640 (Sigma Aldrich, Germany), supplemented with 10% of heat inactivated fetal calf serum (FCS), L-glutamine (100 µg/ml), and gentamycin (20 µg/ml) at 37^{o}C and 5% CO_2. Cell culture media for H929 was additionally supplemented with 0.05 mM of beta-2-mercaptoehtanol and cultured at 8% CO_2. Replacement of fresh medium was regularly done twice weekly at dilution of 1:10/1:20 with growth medium.

The human monocytes cell line THP-1 (purchased from ATCC) were cultured in RPMI-1640 medium containing 10% heat-inactivated fetal calf serum (FCS) adjusted to contain 2mM L-glutamine, 1.5 g/L sodium bicarbonate, 4.5 g/ml glucose, 10mM HEPES and supplemented with 0.05 mM 2-Mercaptoethanol. Cells were maintained in T75 flask at 37.0 C in a humidified atmosphere with 5% carbon dioxide (CO_2). Addition of fresh medium was provided regularly every 2 to 3 days by diluting them 1:2/1:3 with growth medium.

3.3.1 THP-1 cells stimulation

Human monocytic cell line, THP-1 cells were seeded at a density of $0.5x10^6$ cells per well in a 24 well plate (Corning, USA). The cells were stimulated with 30 ng/ml of rhM-CSF (R&D system, USA; catalog 216-MC-025/CF), for 3 days and then used for flow analysis.

3.4 Principle of Flow Cytometry

Flow cytometry-based analysis was extensively used in this project to detect the level of expression of extra and intra-cellular proteins as well as identifying which cells in the bone marrow samples of myeloma patients expressed these proteins. Flow cytometry has the ability to measure not only the level of cytoplasmic and surface molecules but also provide information about the physical properties of single cell in suspension including cell size, shape and density. Flow cytometry is the composite of three efficiently regulated components; *a)* Fluidics system, *b)* Optics and *c)* Signal processing.

The fluidics system is used to load and singularize the sample for analysis. The sample to be analyzed is injected in narrowing conical shaped sample core, within the moving stream of sheath fluid. The moving sheath fluid carries the sample upward to the center in the flow cell creating a drag effect. The gradient increases in the sheath fluid velocity toward the center and creates a single file of cells, intercepted by laser beam is known as hyrdrodynamic focusing (Figure 3.3). The difference between the sample stream and sheath fluid stream pressure is exploited to change the diameter of the sample

core, increasing the sample stream pressure results in to increased sample core diameter, and high flow rate. BD LSR II has been used in this study, in which a belt in air pump provides a sheath fluid pressure of 5.5 psi.

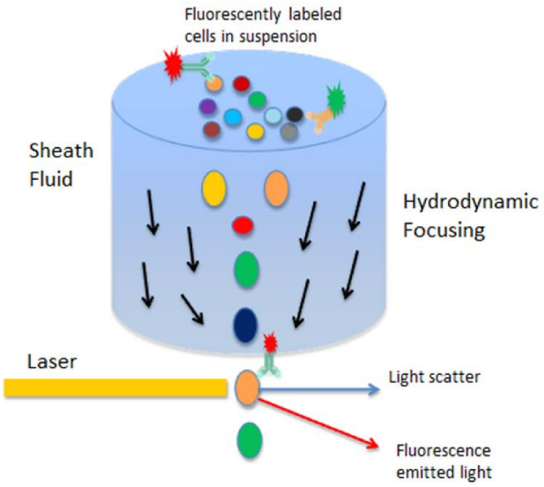

Figure 3.3 The flow cell.

Hydrodynamic focusing allows the cells to be interrogated by the laser one by one. Following sample injection, the cells are randomly distributed into a stream of fluid where a single cell (event) can be interrogated by a beam of monochromatic lights from lasers. * The figure is drawn by the author.

Optics includes lasers, optical filters and detectors and in BD LSR II is equipped with white light, four different lasers of specific wave length (405, 488, 561 and 640) and several optical filters. Detectors detect and record the scattered light and fluorescence emitted from fluorochromes. The light is scattered in all direction after interrogating particles, and the axial scattering is known as forward scattering (FSC) and perpendicular scattering is denoted as side scattering (SSC). Scattering provide information about the physical properties of the particle like FSC tells about the particle size while SSC explains the internal complexity or granularity of the particle (Figure 3.4).

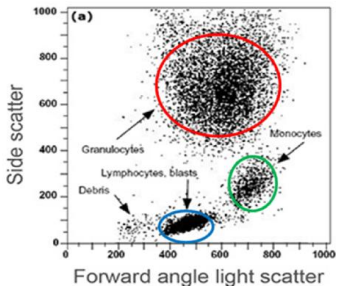

Figure 3.4 A representative flow cytometry dot plot

FSC versus SSC allows discrimination between different populations of cells in human blood sample. Each dot represents a single cell analyzed by the Flow cytometer. The different positions of the cell populations is defined

by differences in cell size (FSC) and granularity (SSC) and thus is it possible distinguishes lymphocytes (blue), monocytes (green), and granulocytes, which are usually large and granular in size (red). (Figure taken from Abcam flow cytometry guide).

Fluorochromes absorb the light of a specific wave length and emit light of another specific wavelength (a bit longer). The light excites electrons that jump from a stable resting state level (S0) to an unstable higher energy state (S1). In this processes the fluorochrome undergoes conformational change, and in doing so, some of the absorbed energy is released as heat. The electrons move back to a lower and stable state level by releasing the remaining energy as fluorescence. The difference between wavelengths of the emission and excitation is called Stokes shift (Figure 3.5).

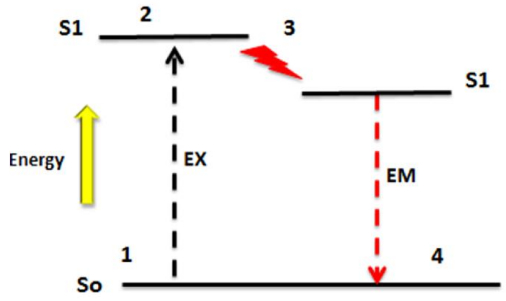

Figure 3.5 Theory of Fluorescence.
When light is absorbed by a fluorochrome electrons move to a high energy state S1, energy loss will occur within a few seconds (3); the electrons fall to a more stable energy level (4) and the remaining energy loss is observed as fluorescence light of a longer wavelength. * The figure is drawn by the author.

Optical filters allow the light of specific wave length to be detected by the detector, above a certain threshold (long pass), below a threshold (short pass) or within a range (band pass). BD LSR II is equipped with only Long pass and band pass optical filters. The selected emission last for a very short duration and is of low intensity and is then amplified and detected by photodiodes or photomultiplier (PMT) (Figure 3.6).
Signaling processing is used for the conversion of scattered light or fluorescence to an electrical signal to be measured or quantified and plotted as dot plot or graphic presentation.

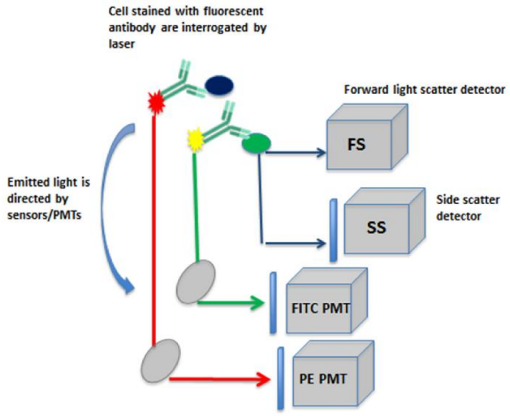

Figure 3.6 Detection and signal processing.

Scattered and fluorescence light is reflected by dichroic mirrors towards filters. Where a specific wavelength is filtered by designed filter and collected by a PMT (detectors). The signal is amplified and converted to electrical signal to be measured or quantified and plotted as graphic presentation. * The figure is drawn by the author.

3.4.1 Compensation, PMT voltage and experimental set up

In modern cytometers, multiple lasers are used to excite multiple fluorochromes. The characteristically colored emissions from each fluorochrome are separated using optical filters. As described above, each detector (FLn) has an optical filter designed to control specificity of detection, allowing only the peak emission of a particular fluorochrome. However practical experience proves that there is still the possibility of fluorescence spillover (Figure 3.7A); it means higher chance that the emission profile of two or more fluorochromes will coincide causing experimental artefacts or false positive signals in other channels. Therefore, spectral overlap between fluorochromes in multicolor experiments requires the use of fluorescence compensation. A single color control was included to set up compensation adjustments for each fluorochrome used in all experiments. Commercially available kits for compensation control (BD™) comprises polystyrene microbeads (3.0-3.4um), including compensation beads used as negative control (unstained cells) and compensation beads coated with anti-mouse Ig k antibodies, with binding capability for any mouse light chain. The microbeads were stained for 20 minutes at room temperature using the same antibodies (each antibody separately), at the same dilution used in the experiment. The background fluorescence from negative control beads will establish basal threshold PMT voltage of the machine. The single fluorochrome stained beads is used by the cytometer to correct the spill-over in multi-color flow cytometric analysis (Figure 3.7B). The compensation can be automatically done by BD LSR II instrument or calculated manually by FlowJo 7.6.5 software on uncompensated samples. Automatic instrument and manually compensations were done in this study. A compensation checkup is done weekly by our laboratory to check the instrument performance. Unstained cells were also used in each experiment to check whether there is variation in

FSC/SSC and background fluorescence between experiments. The same instrument settings were used for all the patient samples.

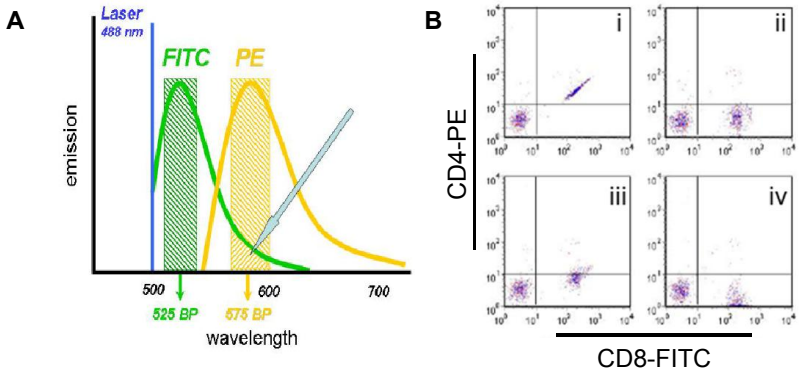

Figure 3.7 The effect of compensation on FITC spillover in to PE channel.

The emission spectra from FITC and (PE) with two bandpass filters are superimposed (A). The long emission spectrum tail of FITC is overlapped with PE channel (arrowed). Human peripheral blood lymphocytes labelled with CD8-FITC showing the $CD4^-$ cells only (B). (i) Uncompensated data. (ii) Correctly compensated. (iii) Under compensated. (iv) Over compensated. (Figure adopted from http://flowbook.denovosoftware.com/chapter-5-immunofluorescence-and-colour-compensation)

3.5 Extra-cellular staining of unseparated bone marrow cells

Freshly collected bone marrow aspirates from myeloma patients were used for multicolor flow cytometeric analysis. Antibodies to CD19, CD3, CD14, HLA-DR and CD66b, were used to stain bone marrow cells and anti-RANK was used both on bone marrow cells as well as M-CSF stimulated THP-1 cells (reagent and antibodies information are enlisted in table 3.2 and appendix V & VII). The bone marrow aspirates (100-200 µl) or $0.5x10^6$ cells were used per sample for staining. The samples were washed in FACS buffer (0.1% BSA in PBS pH 7.2) and centrifuged at 448 g for 5 minutes. The supernatant was discarded and the cell pellets were re-suspended in 50 µl of FACS buffer. In order to inhibit non-specific Fc binding of antibodies, Fc receptors were blocked by adding 20 µl of human Fc receptor block solution for 20 minutes on ice. The cocktail of antibodies at indicated dilutions were then added to the samples and incubated for another 30 minutes on ice in the dark. The samples were washed and centrifuged at 448 g for 5 minutes and supernatant was discarded. Streptavidin conjugated fluorochrome was added to biotin-conjugated antibodies for detection (as indicated in the Table 3.2). The samples were washed in FACS buffer twice to remove un-bound antibodies and subjected to 1-step Fix/lysis solution (diluted 1:10 in dH_2O) incubation for 5 minutes. The 1-step Fix/lysis solution contains 4% PFA for fixation as well as an ammonium chloride reagent that simultaneously lyses the red blood cells (RBCs). The samples were then washed in FACS buffer (1 ml) and centrifuged at 448 g for 5 minutes. The optimum dilutions of antibodies used in this study was determined by titrating the

antibodies (Table 3.2). Flourescence minus one (FMO) as well as mouse IgG1 isotype antibodies was used as negative control for anti-RANK staining. The FMO sample was stained with all the conjugated antibodies used in the test samples except anti Rank-PE. The FMO control is now commonly used as negative controls in multicolor (3 or more colors) flow analysis rather than an isotype controls, as it reduces background staining due to fluorescence spillover. In most people's experience the isotype controls have been found not useful due to their limitations such as background staining and, in addition, they do not account for fluorescence spillover and therefore less appropriate in multicolor flow cytometric analysis [79].

Table 3.2 Antibodies used for extra-cellular staining of unseparated bone marrow cells

Antibodies	Fluorochorme	Dilution (µl/sample)	Vendor
CD66b	FITC	10	BD Pharmingen
CD14	PECy7	2.5	BD Pharmingen
RANK	PE	10	R&D Systems
HLA-DR	V450	5	eBioscience
CD-3-biotin	-	5	eBioscience
CD19-biotin	-	5	eBioscience
Streptavidin*	APC-Cy7	1:500 (dilution factor)	BD Pharmingen

*Streptavidin: Streptavidin not antibodies but a protein that has high affinity for biotin and here is conjugated with APC-Cy7

Table 3.3 Antibodies used for extra-cellular staining of separated bone marrow cells

Antibodies	Fluorochrome	Dilution (µl/sample)	Vendor
CD38	PE-Cy7	2.5	BD Biosciences
CD45	V500	2.5	BD Biosciences
CD19	APC-H7	2.5	BD Biosciences
CD14	BV510	2.5	BioLegend
CD3	PerCP-Cy5.5	2.5	eBioscience

3.6 Intra-cellular staining of separated bone marrow cells

Separated patient $CD138^+$ plasma cells and CD138 negative fractions were surface stained with a cocktail of anti CD38 and CD45, or a cocktail of anti CD19, CD14, and CD3, respectively, fixed with paraformaldehyde (PFA) and then subjected to intra-cellular staining for IL-32 (regents and antibodies information are enlisted in table 3.3 & 3.4 and appendix V & III). The optimum dilutions of antibodies

used for surface staining in this study was determined by titrating the antibodies. After cell surface staining the bone marrow cells or myeloma cell lines ($1.0x10^6$ cells/samples) were washed with PBS and centrifuged at 448 g for 5 minutes. The samples were fixed with PFA (2% in PBS) for 20 minutes at room temperature and then washed with PBS twice. The cells were permeabilized with 500 µl of permeabilization buffer (0.5% saponin in FACS buffer) for 5 minutes and then centrifuged at 448 g for 5 minutes. The supernatant was discarded while cells were stained with Anti-goat IL-32 antibodies or normal goat IgG (diluted 1:100 in washing buffer) for 30 minutes at room temperature. The cells were washed twice with washing buffer (0.1% saponin in FACS buffer) and then incubated with alexa-488 conjugated secondary antibodies (diluted 1:1000 in washing buffer) for 30 minutes at room temperature. The samples were washed twice with washing buffer to remove the unbound antibodies and once with FACS buffer to remove saponin and then re-suspended in 400 µl of FACS buffer for flow cytometric analysis.

Table 3.4 Antibodies used for intra-cellular staining

Antibodies	Fluorochrome	Dilution	Vendor
Goat IL-32**	-	1:100	R&D Systems
Anti-goat	Alexa-488	1:1000	Invitrogen
Normal goat IgG	-	1:100	Santa Cruz

** Anti-IL-32 is un-conjugated goat anti-human polyclonal antibodies.

3.7 Flow cytometric analysis

Samples, re-suspended in FACS buffer (400 µl) were acquired on BD LSR II Flow cytometer. Approximately 50000-100000 events were recorded with FACS Diva software (Becton Dicknson). Data were subsequently analyzed with FlowJo software 7.6.5 (TreeStar, Ashland, OR, USA).

3.8 Statistical analysis

All data analysis and graphical representation of data was performed using GraphPad Prism. The Wilcoxon matched-pairs signed rank test was used for statistical differences in receptor expression between $RANK^+$ monocytes and $RANK^+$ granulocytes and bar on the graph shows the median of $RANK^+$ cells. We performed linear regression to show relationship between groups and spearman's test to show significance correlation (P value) between groups. Mann-Whitney t-test was used to determine statistical differences in the median fluorescence intensity (MFI) of RANK expression on monocytes and granulocytes as well as FMO controls. In all cases, results were considered significant at $p<0.05$. The median fluorescence intensity was calculated rather than the mean fluorescence intensity because the median is more representative and less affected by outliers or skew, as a right-hand skew of data may cause even more overestimation of the mean values.

4 Results

4.1 Determining RANK expression on granulocytes in the bone marrow of myeloma patients

Osteoclastic bone destruction is a common complication in MM patients, due to abnormal bone remodeling process with enhanced osteoclast activity and suppressed osteoblast function. RANK and its ligand RANKL are potential inducers of bone resorbing osteoclasts. RANK is commonly found as a surface receptor on osteoclast precursors [54], which are believed to arise from monocyte progenitors usually resident in the bone marrow as well as from circulating monocytes [80]. However, only a minor fraction (1-2%) of peripheral blood monocytes expressing RANK are committed to differentiate into osteoclasts [81]. Moreover, RANK is not only a receptor for monocytes. Studies conducted on normal PB and BMMNCs, reported RANK expression on various populations in the bone marrow [81]. Literature reported that monocytes, granulocytes as well as osteoclast precursors share common progenitors and similar effector function, as reflected in their expression of several common surface markers (e. g. CD14, CD11b). It is therefore possible that granulocytes or a population of granulocytes could differentiate into osteoclasts.

Recently researchers have found an increase expression of RANK on a population of granulocytes derived from patients with bacterial infections as well as in rheumatoid arthritis when compared with healthy donors. These cells had also the potential to differentiate into osteoclasts [82]. Therefore, we wanted to find out whether a population of granulocytes expresses RANK and whether these could be identified in the bone marrow of myeloma patients. In order to investigate the expression of RANK on granulocytes and monocytes in myeloma bone marrow cells we used multicolor flow cytometric analysis on un-separated bone marrow cells stained with a panel of antibodies that would allow us to define distinct cell types including monocytes and granulocytes. We used a combination of antibodies to characterized specific cell surface markers including CD14 for monocyte detection and CD66b for granulocytes, with CD3, CD19 (T cells and B cells respectively) to further remove T cells and B cells from the analysis, in combination with anti-RANK. Anti-HLA DR was included in the panel as a further marker to distinguish the two cell populations as granulocytes are generally HLA DR^- and $CD14^-$ and monocytes HLA DR^+ $CD14^+$.

4.1.1 RANK expression is detectable on the monocytic cell line THP-1 cells after stimulation with recombinant M-CSF

It was necessary to test the specificity and sensitivity of anti-RANK-PE antibodies to be used for the Flow cytometric analysis. As RANK is expressed on the peripheral blood monocytes after stimulation with M-CSF [83, 84], a human monocytic cell line THP-1 was exposed for 3 days to 30 ng/mL of M-CSF (as described in the material and methods section), and stained with PE conjugated anti-RANK antibodies as well as isotype control. Staining of THP-1 cells was performed with a new batch and an old batch of anti-RANK antibodies and isotype control (Figure 4.1). Gates were set on live cells with FSC versus SSC. (Figure 4.1*A*). Our flow cytometric analysis showed that RANK was detectable on the surface of THP-1 cells after M-CSF stimulation, since staining with both anti-rank antibodies showed a higher proportion of cells that stained positive with anti-RANK antibodies than with isotype control as well as an increased median fluorescence intensity (MFI) compared to control isotype antibody. On note, both antibodies stained a similar proportion of cells as the analysis showed that 21.6% of the cells were $RANK^+$ when stained with old antibodies and 20.1% when stained with new antibodies (Figure 4.1*B* and *C*). Collectively, in our experiment, we could detect surface RANK on THP-1 cells and the anti-RANK could be used to determine RANK expression on bone marrow cells.

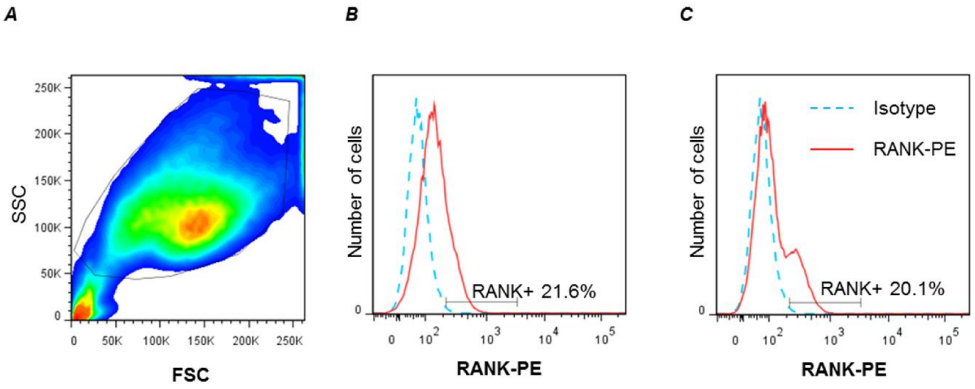

Figure 4.1 RANK expression on monocytic cell line THP-1 cells.
Human monocytic THP-1 cells were stimulated in the presence of M-CSF (30 ng/ml) for 3 days and stained with two different batches of anti-RANK-PE antibodies or isotype. The stained cells were analyzed on an LSR II Flow cytometer for RANK expression. (*A*) THP-1cells were gated on live cells with FSC versus SSC (right panel). Percentage of $RANK^+$ cells on the gated cells for old anti-RANK (*B*) and (*C*) new anti-RANK. Isotype control was used as a negative control (blue dotted line).

4.1.2 Gating strategy and identification of granulocytes and monocytes in the bone marrow

To detect the expression of RANK on monocytes and on granulocytes present in the bone marrow of myeloma patients, un separated bone marrow cells from patients suffering from multiple myeloma were stained, as mentioned above, with a panel of antibodies against distinct surface markers, lineage (CD3, CD19), CD14, HLA DR and CD66b. Therefore, we set out to determine RANK on monocytes and granulocytes. Monocytes were identified as lineage$^-$, CD66b$^-$, HLA DR$^+$, CD14$^+$ and granulocytes as lineage$^-$, CD66b$^+$, HLA DR$^-$, and CD14$^-$. Our gating strategy for the identification of bone marrow derived-myeloid cell subsets is illustrated in Figure 4.2. Monocytes and granulocytes were identified in the bone marrow and gates were set on live cells with FCS versus SSC and doublets were excluded. Lineage cells (CD3$^+$, CD19$^+$) were further gated out (Appendix IA) and monocytes identified as CD14$^+$, CD66b$^-$ cells, and granulocytes as CD66b$^+$, CD14$^-$ cells. We found out that gated monocytes were HLA DR$^+$ and the gated granulocytes HLA DR$^-$ (Appendix IB). The dot plot of CD14 versus CD66b cells from a representative patient is shown (Figure 4.2 upper panel). The percentage of RANK$^+$ cells were further determined on the gated populations (monocytes and granulocytes) as shown in the histogram plots (Figure 4.2 lower panels). FMO control, containing the antibody cocktail except anti-RANK, was used as negative control to set the histogram gate (dotted line) in order to determine the percentage RANK$^+$ cells as well median of fluorescence intensities (MFI) on the RANK$^+$ cells.

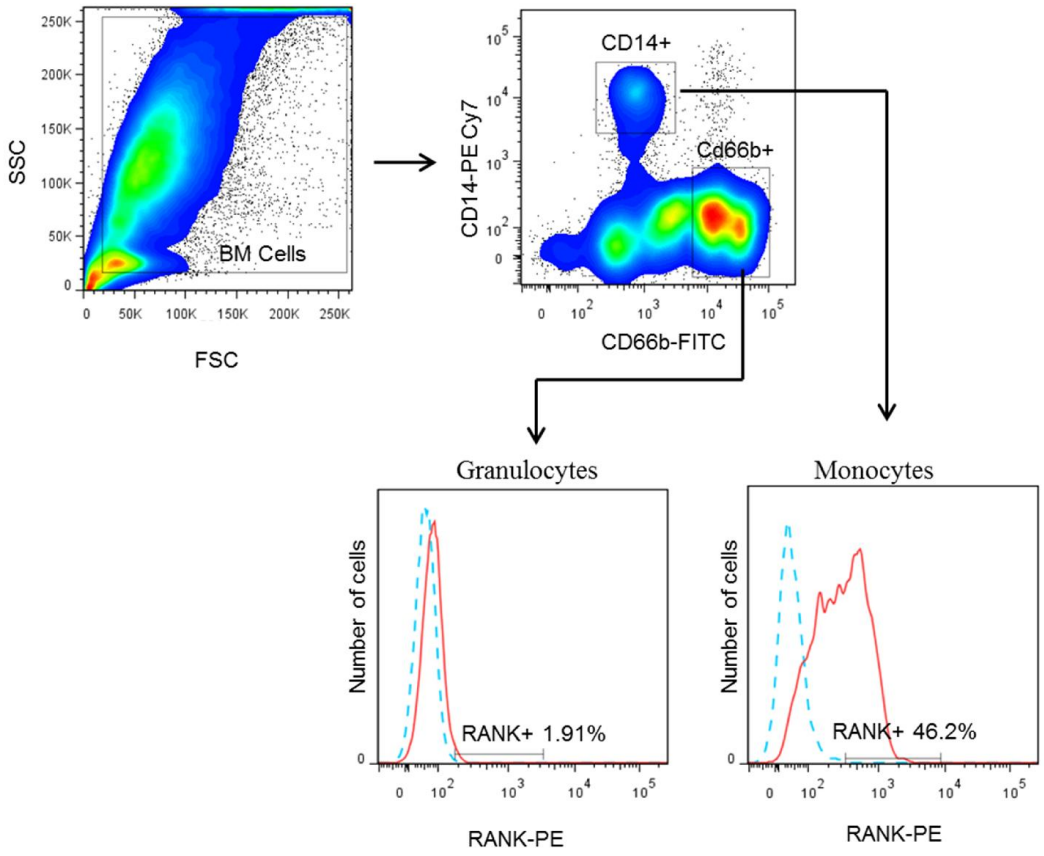

Figure 4.2 Gating strategy for the identification of granulocytes and monocytes.
Unseparated bone marrow cells were co-stained for RANK and a cocktail of antibodies against surface markers, lineage (CD3, CD19), CD14, HLA DR and CD66b before analysis on LSR II Flow cytometer. Gate were set on live cells with FSC versus SSC (upper left panel), and doublets were excluded. Lineage cells (CD3, CD19) were further excluded. Dot plot of CD14 versus CD66b staining from a representative patient is shown (upper panel). Monocytes were gated as $CD14^{+}$, $CD66b^{-}$ and granulocytes as $CD66b^{+}$ (upper left panel). Histogram plots (lower panels) show the percentage of $RANK^{+}$ cells on the gated populations (monocytes and granulocytes) (lower panels). FMO (fluorescence minus one) was used as a negative control (blue dotted line).

4.1.3 RANK expression on myeloid cells in the bone marrow of myeloma patients

Using the gating strategy described in Figure 4.2, we set out to determine whether granulocyte such as $CD66b^{+}$ granulocytes cells express RANK on their surface. We determined the fractions of $RANK^{+}$ monocytes and granulocytes in the bone marrow aspirates. Figure 4.3 shows histograms of RANK expression of the gated $CD14^{+}$ and $CD66b^{+}$ cells. The percentage $RANK^{+}$ cells is determined by setting the gate on FMO control and shown on the histogram. RANK expression in three different patients is depicted. Patient ***(A)*** had high percentage of $RANK^{+}$ monocytes, patient ***(B)*** intermediate percentage and patient ***(C)*** low or no $RANK^{+}$ monocytes. Very few $CD66b^{+}$ granulocytes from these three patients expressed RANK (Figure 4.3), even the patient with 46.2% $RANK^{+}$ monocytes (Figure

4.3***A***) had only 1.91% $RANK^+$ granulocytes. Both patients, who had an intermediate proportion of $RANK^+$ monocytes and patient ***(C)*** with very low/no $RANK^+$ monocytes, had very few $RANK^+$ granulocytes. Patient ***(C)*** where only, 1,01% of monocytes were positive for RANK, had 0,206% $RANK^+$ granulocytes, similar to what was observed in patient ***(B)*** who had more (19,2%) $RANK^+$ monocytes.

We extended the study and included more patients (Table 4.1). Our results indicated that the proportion of $RANK^+$ cells varied between the myeloma patients (Table 4.1 and Figure 4.4 left panel) ranging from less than 1% to above 40% on $CD14^+$ monocytes. Five of the patients, showed an increased proportion of $RANK^+$ monocytes (above the median value), five similar to the median, while the rest (4/14) were have low percentage (below the median) of $RANK^+$ monocytes. We found significantly fewer $RANK^+$ granulocytes than $RANK^+$ monocytes in the bone marrow of the myeloma patients (Figure 4.4 left panel $p< 0.002$), and no significant correlation between the proportion of $RANK^+$ granulocytes and $RANK^+$ monocytes (Figure 4.4 right panel), which indicate that patients with high proportion of $RANK^+$ monocytes do not have a lot of $RANK^+$ granulocytes. Collectively our data indicated that the majority of patients were observed to have low or no $RANK^+$ monocytes. However, Figures 4.3 ***A***, ***B*** and ***C***, showed that marrow $CD14^+$ monocytes are still the most likely source of osteoclast precursors [51, 60], while osteoclast precursors may not be abundant in the $CD66b^+$ granulocyte fraction of patient's bone marrow.

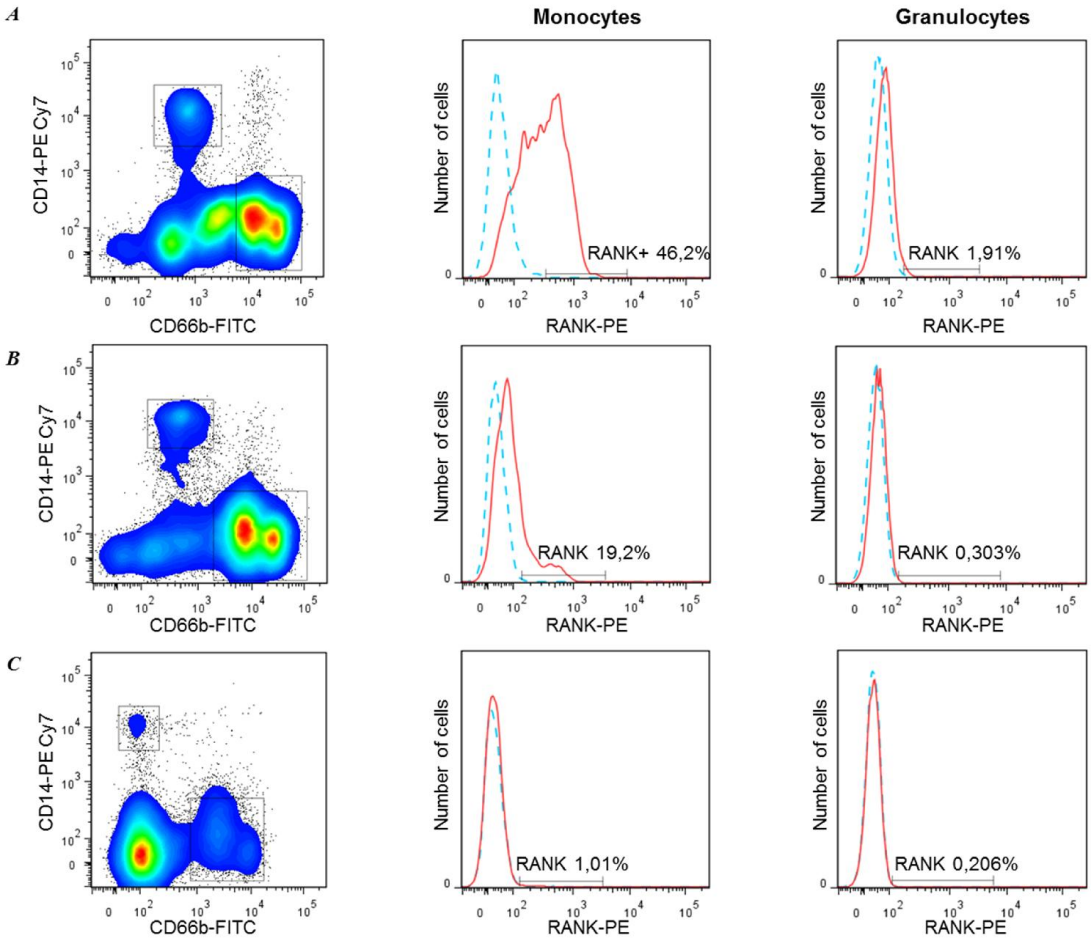

Figure 4.3 RANK expression on gated monocytes and granulocytes in the bone marrow of myeloma patients.
Bone marrow cells were co-stained for RANK and antibodies against lineage (CD3, CD19), HLA DR, CD14, and CD66b. Gates were set on live cells with FSC versus SSC, doublets and $CD3^+$, $CD19^+$ cells were excluded. Dot plots of $CD14^+$ monocytes and $CD66b^+$ granulocytes are shown (left and middle panels). RANK staining on monocytes (middle panels) and granulocytes (left panels) in three different patients is presented. Patients were grouped as high ***(a)***, intermediate ***(b)***, and ***(c)*** low $RANK^+$ cells. Histogram plots show the percentage of $RANK^+$ monocytes (middle panels) and granulocytes (left panels). Gates were set as described in (Figure 4.2). Fluorescence minus one (FMO) was used as a negative control (blue dotted line in each histogram).

Table 4.1 summarizes the percentage of RANK positive monocytes, granulocytes and %PC in patient bone marrow smears

Patient ID	RANK+ Monocytes (%)	RANK+ Granulocytes (%)	%PC (Smear)
1540	0.934	0.287	X
1542	1.08	0.342	X
1544	1.72	0.341	2
1490	1.05	0.341	X
1421	0.37	0.317	X
302	2.57	0.199	30-40
1494	46.2	1.91	38
1500	0.54	0.197	65
1502	1.26	0.312	2
1519	19.2	0.303	X
1539	1.01	0.206	95
1334	0.746	0.251	70
1348	0.358	0.365	X
1349	2.77	0.174	21

x data not available

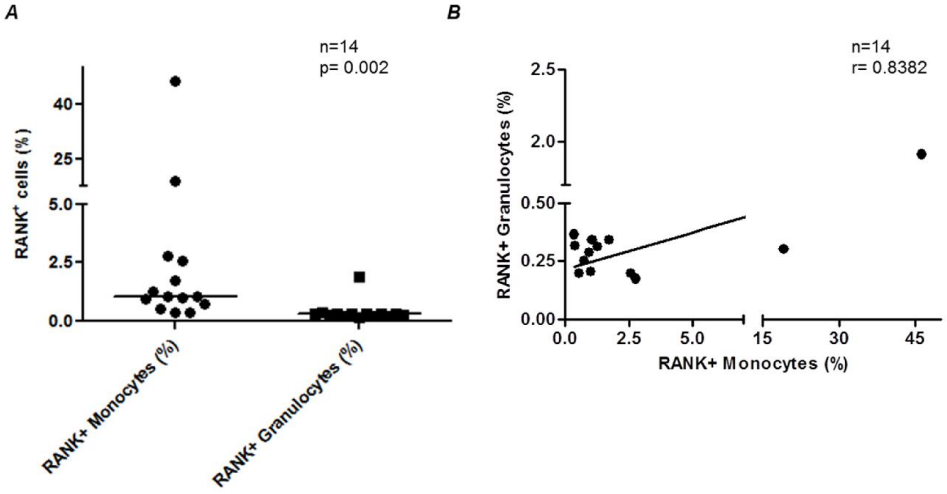

Figure 4.4 Expression of RANK on monocytes and granulocytes in myeloma bone marrow aspirates. Bone marrow samples were co-stained for RANK and antibodies against lineage (CD3, CD19), HLA DR, CD14, and CD66b and analyzed by flow cytometry. Gates were set on FSC and SSC, doublets and $CD3^+$, $CD19^+$ cells were excluded. (A) Distribution of percentage $RANK^+$ monocytes and granulocytes in the bone marrow of patients. P value and significant changes were calculated using Wilcoxon matched-pairs signed rank test. Bars on the graph show the median of $RANK^+$ cells. (B) Correlation of percentage $RANK^+$ granulocytes versus percentage $RANK^+$ monocytes. Each dot represents one patient (n= 14). P value was calculated from a Spearman's test.

Table 4.2 Clinical/laboratory data at diagnosis in multiple myeloma patients

Patient ID	Sex	Age	%PC (Smear)	M COMP. g/L	Subtype	Treatment	Diagnosis	Osteolytic Lesions
1540	F	70	x	x	x	x	x	x
1542	M	73	x	24	IgG k	Untreated	Myeloma	x
1544	M	63	2	8		Untreated	Myeloma	Yes
1421	F	76	x	x	x	x	x	x
302	F	86	30-40	29	IgG k	Treated Earlier	Myeloma Relapse	Yes
1494	M	79	38	8	IgA k	Untreated	Myeloma	x
1500	F	67	65	x	IgG k	Treated	Myeloma	Yes
1502	M	77	2	1/3,5	IgA/IgM	Untreated	MGUS	No
1519	M	68	x	x	x	x	x	x
1539	F	58	95	62	IgA k	Untreated	Myeloma Relapse	Yes
1334	F	53	70		Free lambda	Untreated	Myeloma	Yes
1348	x	x	x	x	x	x	No Myeloma	x
1349	M	66	21	36.3	IgA k	Untreated	Myeloma	x
1490	x	x	x	x	x	x	x	x

x data not available

Table 4.2 shows the patient's clinical data at diagnosis of Multiple Myeloma. Unfortunately, the clinical information are partial as it has been difficult to collect all data from patients who donated bone marrow from other hospital than St. Olavs. The percentage of plasma cells (PCs) in the bone marrow is one of the indicators of tumor load [85]. We observed that the 14 patients had variable tumor loads ranging from low percentage PC (2%) (n= 2), intermediate (20-40%) (n=3), and high (> 40%) (n=3). 6 patients were diagnosed with Multiple myeloma, 1 with MGUS, and 1 did not have either MGUS or Multiple myeloma. Bone lesions are normally present in more than 80% on myeloma patients [25] but the presence of bone lesions was only noted in the journal in 5 of our group of patients. However, due to difficulties in obtaining all the clinical information, more of the patients may have bone lesions. Recent evidence and our clinical data (Table 4.2) indicate that there is a relationship between a patient's tumor burden and presence of lytic lesions and tumor load [42]. Therefore, we also asked whether there was a correlation between the proportion of $RANK^+$ monocytes and $RANK^+$ granulocytes in patients with high percentage PC (Figure 4.5 *A* and *B*). No significant correlation was observed with increased percentage of PCs and the proportion of $RANK^+$ monocytes and $RANK^+$ granulocytes, since very fewer $RANK^+$ monocytes/granulocytes were observed in patients with increased tumor load (Table 4.1 and Figure 4.5A and B). In the light of these data no or very few $RANK^+$ granulocytes were detected even in the patients that had a lot of RANK on their monocytes.

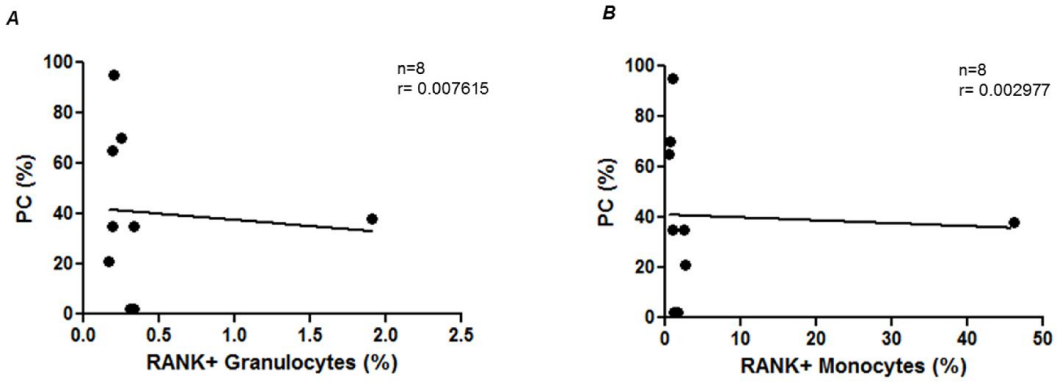

Figure 4.5 Correlation of RANK+ positive monocytes and granulocytes with tumor load.

The percentage $RANK^+$ monocytes and granulocytes versus percentage bone marrow plasma cells (*A-B*) as determined by flow cytometry. The figures show that the proportion of $RANK^+$ monocytes and granulocytes does not increase with tumor load. Each dot represents one patient (n= 14). P values were calculated from a Spearman's test.

4.1.4 Identification of RANK$^+$ granulocytes within CD66b positive subpopulations

Osteoclast precursors may not be abundant in the human blood or bone marrow [86]. In addition it was found that only a population of granulocytes could differentiate into osteoclasts [82]. We therefore wanted to investigate whether RANK$^+$ granulocytes could be detected within sub populations of CD14$^-$, CD66b$^+$ granulocytes. The granulocytes exhibited quite different levels of the CD66b surface marker. Some patients had one, others two or 3 populations with different levels of CD66b (Examples of such dot plots are shown in patient 1 and 2 Figure 4.6). The various granulocyte populations, CD66b^{low}, CD66b^{mid}, CD66b^{high} expressing cells, were denoted by a, b, c, respectively. RANK$^+$ granulocytes were further quantified on the gated populations (a, b, c), as shown in the histogram plots (Figure 4.6). A threshold was defined with FMO (control). By applying this gating strategy we found RANK$^+$ granulocytes in only 1 of the patients (patient 1494) (Table 4.3, Figure 4.6). This patient had three sub-populations of RANK$^+$ granulocytes (a, 3.46%), (b, 7.12%) and (c, 6.99%) and higher then median percentage. We could detect no or very few (below than median) RANK$^+$ granulocytes, in any of the other 13 patients. Collectively our data shown in Table 4.3, and Figure 4.6, indicated very fewer RANK$^+$ cells within sub populations of CD14$^-$ and CD66b$^+$ granulocytes.

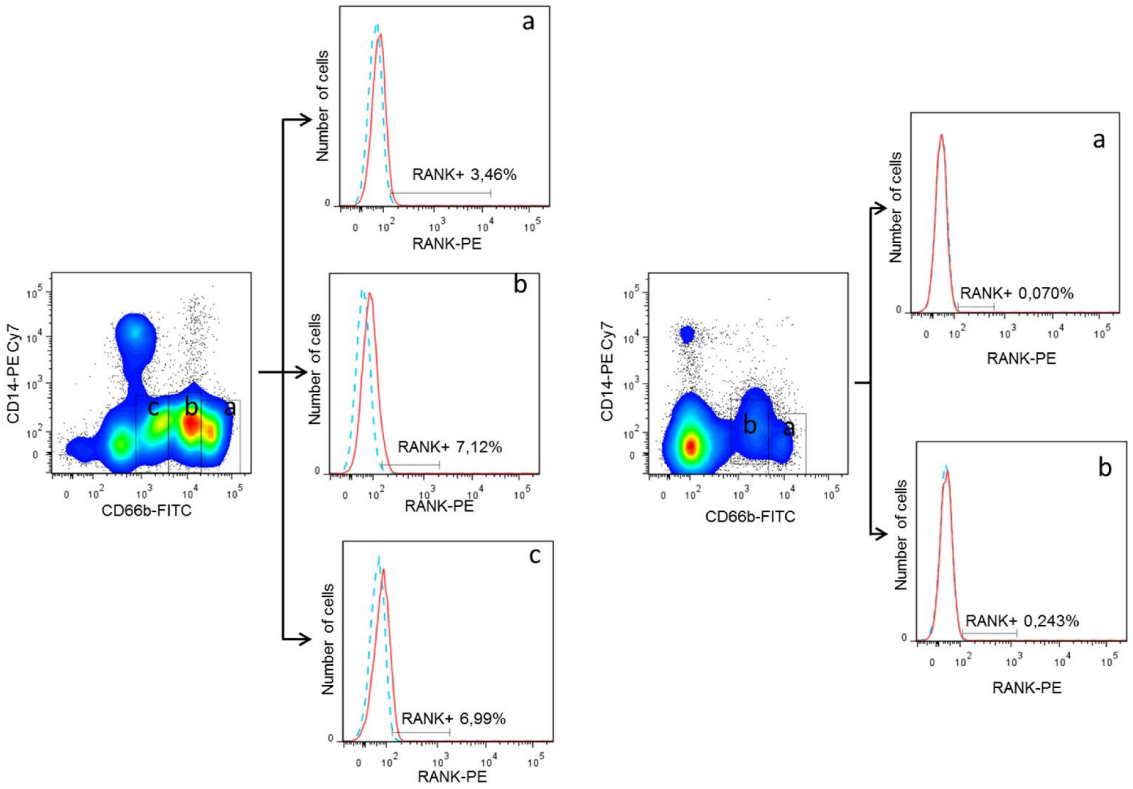

Figure 4.6 RANK expression within subpopulation of CD66b positive granulocytes.

Unseparated bone marrow cells were co-stained for RANK and a cocktail of antibodies against surface markers, lineage (CD3, CD19), CD14, HLA DR and CD66b before analysis on LSR II Flow cytometer. Gate were set on live cells with FSC versus SSC (upper left panel), doublets were excluded. Lineage cells (CD3, CD19) were further excluded. The gates indicated in the dot plots (left and right panels) show granulocytes populations with $CD66b^{low}$ (c), $CD66b^{mid}$ (b) and $CD66b^{high}$ (a). Histograms of RANK staining on subpopulation of granulocytes (middle and left panels). The percentage indicated $RANK^{+}$ granulocytes on the gated populations (a, b, c). (FMO) fluorescence minus one was used as a negative control. The staining shown is representative of cells from 14 patients.

Table 4.3 Summarizes the RANK expression on CD66b positive granulocytes subpopulations determined on all 14 patients

Patient ID	a (%) RANK	b (%) RANK	c (%) RANK
1540	-	0.264	-
1542	0.102	0.436	-
1544	0.056	0.364	-
1490	0.2	0.532	0.113
1421	1.02	0.519	0.434
1494	3.46	7.12	6.99
1500	-	0.43	0.65
1502	0.375	1.26	0.523
302	0.675	0.217	0.407
1519	0.303	2.03	0.449
1539	0.07	0.262	-
1349	-	0.507	-
1348	0.551	0.854	-
1349	0.507	0.507	-

4.1.5 Level of RANK expression on monocytes and granulocytes in the bone marrow of myeloma patients

The number of $RANK^+$ osteoclast precursors is reported to be important for the development of bone disease [32] but the amount of RANK on the precursors may also be important. We therefore determined the level of RANK expression on $CD14^+$ monocytes and $CD66b^+$ granulocytes by measuring MFI (median fluorescence intensity) on both cell populations. In this analysis we determined the MFI on $RANK^+$ cells (gates set on FMO control). Our results indicate no noticeable differences in the level of RANK expression on monocytes compared to the RANK expression on granulocytes. Most of the patients were found to have similar level of RANK expression (below or just above the median) in both cell populations (Figure 4.7). Although, one patient (1/14), expressing high levels of RANK (MFI 300) on monocytes, had very low levels of RANK on the $CD66b^+$ granulocytes.

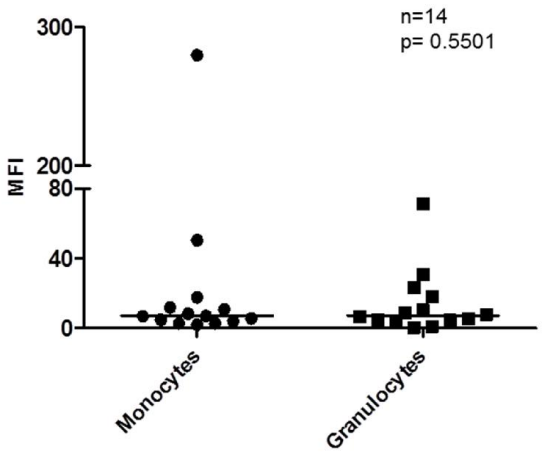

Figure 4.7 Comparison between the level of RANK expression on monocytes and granulocytes in myeloma patient's bone marrow.

The level of RANK expression is measured in median fluorescence intensity (MFI) and determined by flow cytometry. No significant differences were observed in the level of RANK expression on monocytes compared to granulocytes. Each dot represents one patient. Statistical differences between groups and controls were done using Mann- Whitney Test. Data are presented after normalization with FMO control. Bars represent the median.

4.1.6 Summary of RANK staining

Collectively our results indicated fewer osteoclast precursors from these patients's bone marrow. We observed that the proportion of $RANK^+$ varied among patients as we found patients with low, intermediate and high monocytes expressing RANK. We found myeloma patients with significantly fewer $RANK^+$ granulocytes than $RANK^+$ monocytes. No significant correlation was found between the proportion of $RANK^+$ monocytes and $RANK^+$ granulocytes in patients with increased tumor load and presence of bone lesions.

4.2 Determining IL-32 expression on bone marrow cells in myeloma patients

Preliminary experiments in our lab showed that IL-32 was expressed by myeloma cell lines and plasma cells from myeloma patients when measured by qPCR and Nanostring analysis, respectively. Our group also showed that IL-32 can also be detected in blood and bone marrow plasma of myeloma patients. In light of the above mentioned, we set out to determine expression of IL-32 protein in myeloma cell lines and bone marrow cells from patients by flow cytometry.

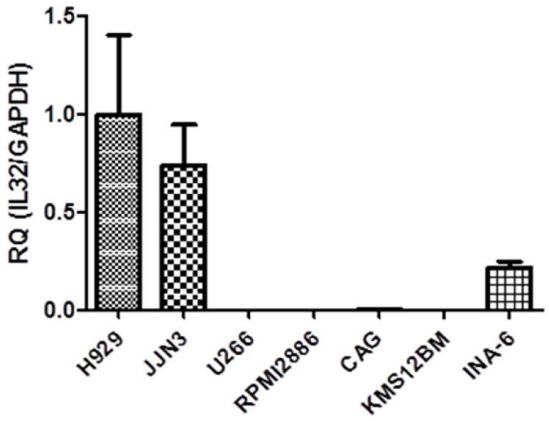

Figure 4.8 IL-32 expression in myeloma cell lines.
mRNA was isolated from Myeloma cell line and subjected to cDNA synthesis. IL-32 expression was evaluated by qPCR and normalized to GAPDH. The graph represents average of three independent replicate and bars represent standard deviation. The results shown here are provided by Therese Standal's group.

4.2.1 Flow cytometric analysis shows intracellular IL-32 expression in myeloma cell lines

In order to test whether myeloma patients have cells that express IL-32, we proceed to stain for intracellular expression of IL-32 and to optimize the staining protocol using myeloma cell lines JJN3 and H929, which expressed IL-32 mRNA level. CAG cell lines were also used as a negative control as did not express intracellular IL-32. As described in materials and methods, we chose a goat anti IL-32 antibodies and Alexa 488 conjugated donkey anti-goat secondary antibodies. Our flow cytometric analysis showed that intracellular IL-32 was detectable on myeloma cell lines (JJN3 and H929 respectively) after incubation with a donkey anti-goat IgG conjugated to Alexa 488, since IL-32 staining showed an increased shift compared to the IgG isotype control or anti-goat IgG Ab alone (Figure 4.8 lower histograms). For the analysis gates were set on live cells (with FSC versus SSC). Then, the gated population was checked for IL-32 expression (Appendix II). When gates were set on the isotype control (Figure 4.8 lower panels) 89.9% of JJN3 and 25.8% of H929 cells expressed IL-32 whilst CAG cells did not express IL-32. Using the same experimental conditions and antibody concentration, similar results were also observed by confocal microscopy by using a 63x oil immersion objective (Figure 4.10). Figure 4.9 illustrates IL-32 specific intracellular labeling of

myeloma cell lines JJN3, H929 and CAG. However, the flow data, supported by confocal images (Figure 4.9 and Figure 4.10), indicated that there were more IL-32^{+} cells in JJN3 cells compared to H929 and no IL-32 expressing cells were found in CAG cells. Collectively, in our experiments we detected intracellular IL-32 on myeloma JJN3 and H929 cell lines, suggesting that we had the correct experimental conditions and antibody concentrations which would allow us to further investigate the presence of IL-32 in myeloma patients.

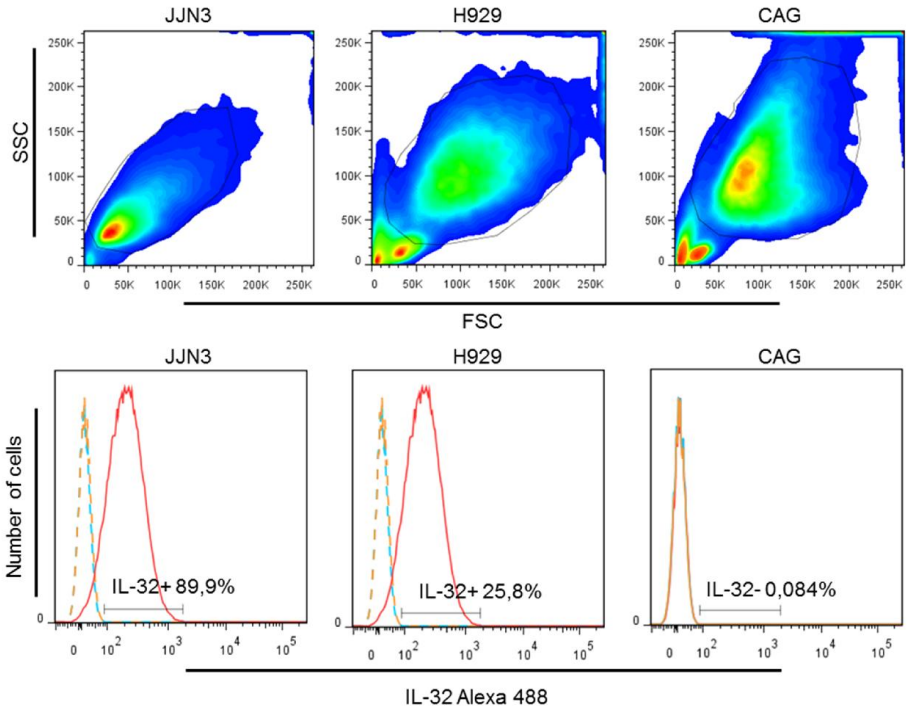

Figure 4.9 IL-32 expression in myeloma cell lines JJN3, H929 and CAG.
Three different myeloma cell lines were fixed and stained with anti-IL-32 antibodies or isotype control as well as anti-goat IgG Alexa 488-conjugated secondary antibodies, before analysis by LSR II flow cytometer. Gates were set on live cells with FSC versus SSC (upper panels). The histograms of IL-32 staining of the gated populations (lower panels). The percentage indicated IL-32^{+} cells on the gated populations (lower panels). Isotype control and anti-goat IgG were used as a negative control (blue and yellow dotted line). Data are representative of 3 independent experiments.

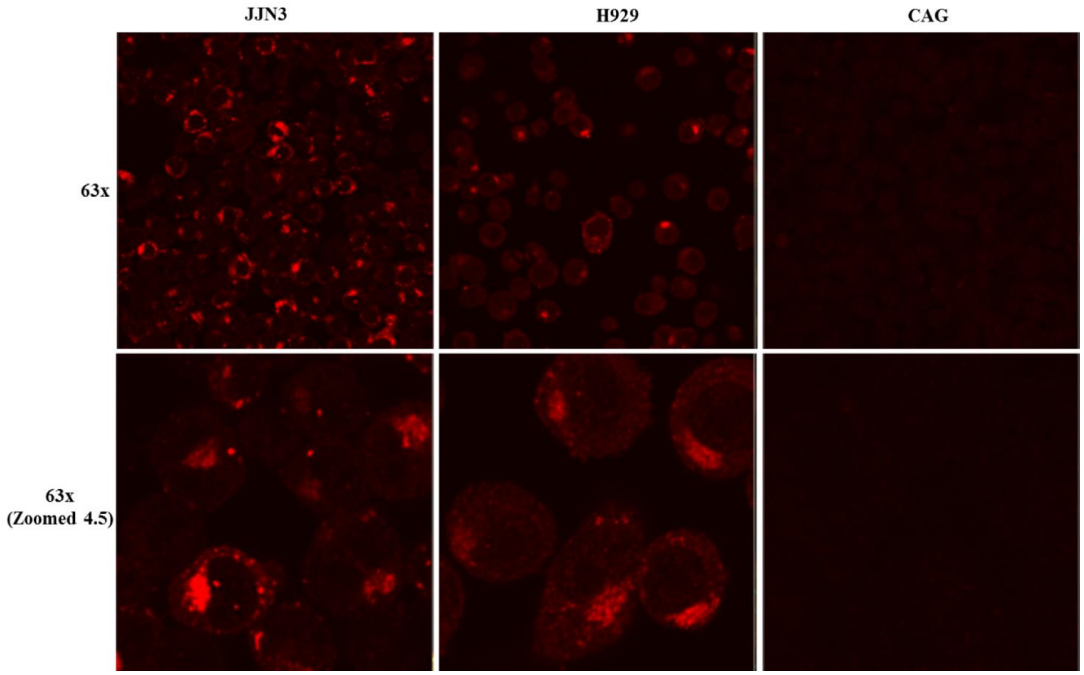

Figure 4.10 Intra-cellular IL-32 in myeloma cell lines.
Three myeloma cell lines, JJN3, H929 and CAG were stained for IL-32 and images for obtained using Zeiss LSM 510 Meta confocal microscope. The zoomed images are presented in lower panel. The results shown here are provided by Therese Standal's group.

4.2.2 IL-32 expression in the bone marrow cells in myeloma patients

4.2.3 A. IL-32 expression in enriched CD138$^+$ plasma cells

In order to determine whether myeloma patients have cells that express IL-32, we used CD138$^+$ enriched plasma cells, as Nanostring analysis (Figure 4.11) were done in enriched plasma cells rather than un-separated bone marrow cells. Enriched CD138$^+$ cells were obtained from 4 patients with diagnosed Multiple myeloma. Purity of enriched CD138$^+$ plasma cells post enrichment was reported to be above 90%. Thus, enriched CD138$^+$ plasma cells were stained for intracellular IL-32 and analyzed by flow cytometry as described in materials and methods. We used a goat anti IL-32 antibodies and Alexa 488 conjugated donkey anti-goat secondary antibodies.

In Figure 4.12 gates were set on FSC versus SSC on cells from 4 patients. Histograms of IL-32 expression of gated cells are shown (Figure 4.12). Isotype matched antibodies (dotted line) were used as a negative control, and the percentage IL-32$^+$ cells of the gated population is indicated on the Figure 4.12. Surprisingly, our flow cytometric analysis showed that there were very few intracellular IL-32$^+$ cells in the CD138$^+$ fraction from these patients (Figure 4.12 lower panels) as we only detected small

proportion (1,98%) of CD138^{+} plasma cells expressing IL-32 in one of the 4 patients. The other 3 patients had very little/ no IL-32^{+} cells (Figure 4.12). Thus, no IL-32 expression was detected.

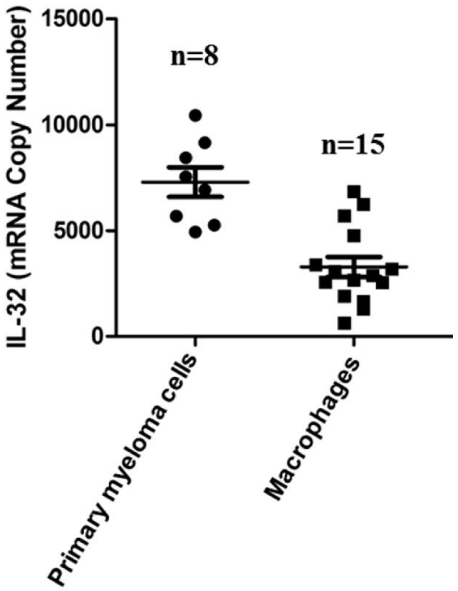

Figure 4.11 IL-32 expression in primary myeloma cells.
mRNA was isolated from CD138^{+} enriched plasma cells from myeloma patients and used for Nanostring analysis. Bone marrow monocytes from myeloma patients were differentiated into macrophages *in vitro*. The results shown here are provided by Therese Standal's group.

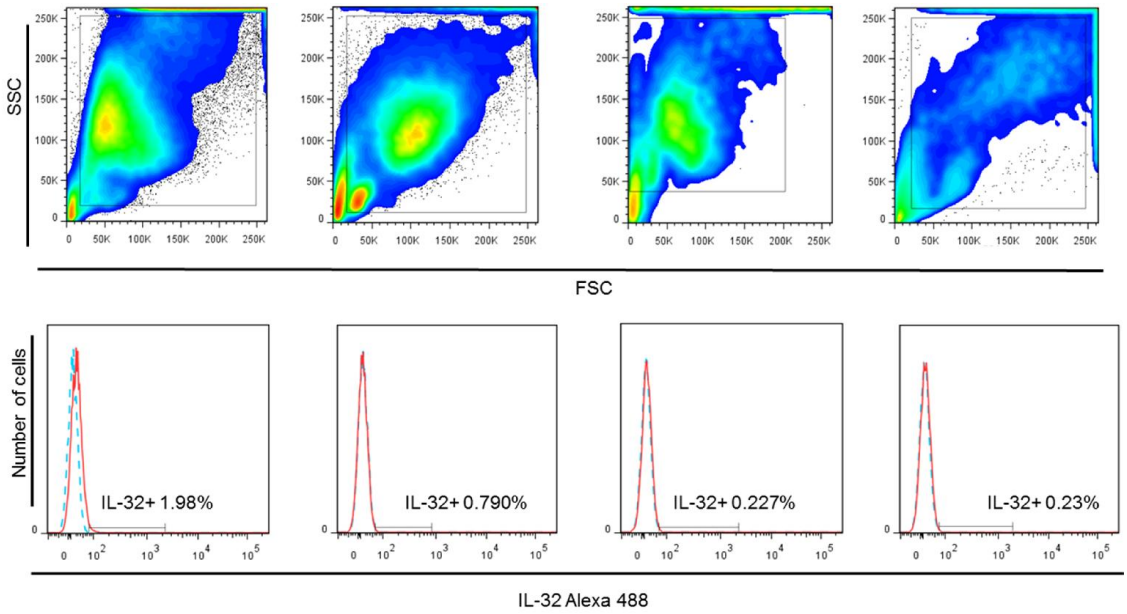

Figure 4.12 IL-32 expression in myeloma CD138^{+} enriched plasma cells.
Enriched CD138^{+} plasma cells were fixed and stained for intra-cellular IL-32 with anti-IL32 or isotype control, and analyzed by LSR II flow cytometer. Gated were set on live cells with FSC versus SSC (upper panels). The

histograms of IL-32 staining of the gated population (lower panels). The percentage of IL-32$^+$ cells of the gated population (lower panels). (n=4) Isotype control was used as a negative control (dotted blue line).

4.2.4 B. IL-32 expression on CD138$^+$ cells with different light scatter properties

Literature reports that MM is a clonally heterogeneous tumor due to its genomic complexity and variable phenotypic profile within the plasma cell population [23, 87]. Although none of the plasma cells from these 4 patients appeared to express IL-32, we could not rule out that a subpopulation of the plasma cells could express and secrete IL-32. Therefore, we found it necessary to identify three or two subpopulation of plasma cells with different light scatter properties by a selective gating strategy as shown in Figure 4.13. Dot plots of distinct subpopulations of the CD138$^+$ plasma cells present in myeloma patients is shown (Figure 4.13 upper dot plots). Although, not surprisingly, the patients had different FSC/SSC patterns, we decided to divide the plasma cells into different subpopulations. Cell that fall into the P1 gate have high SSC and FSC, cells within the P2 gate have medium SSC and high FSC, while small cells with low FSC and SSC were placed in the P3 gate (Figure 4.6 upper dot plots). Histogram plots of IL-32 expressing plasma cells of the gated subpopulations from the 4 patients are shown (Figure 4.13 lower panels). In 3 of patients, there was no evidence of a subpopulation of plasma cells expressing IL-32. Interestingly, one patient (donor 1675 in Table 4.4) had an increase percentage of IL-32$^+$ plasma cells within the P1, P2 and P3 regions compared with the total gates (FSC, SSC gate in Figure 4.13), indicating that not all plasma cells within the bone marrow of myeloma patients express equal amount of IL-32. In patient 1675 the cells within the P1 gate had 5,94% IL-32$^+$ cells, whilst 2,41% and 2,59% IL-32 producing cells were found in the P2 and P3 gates respectively (Figure 4.13 lower left panels). In contrast, in the other 3 patients IL-32 expression was low or absent on the CD138$^+$ fraction.

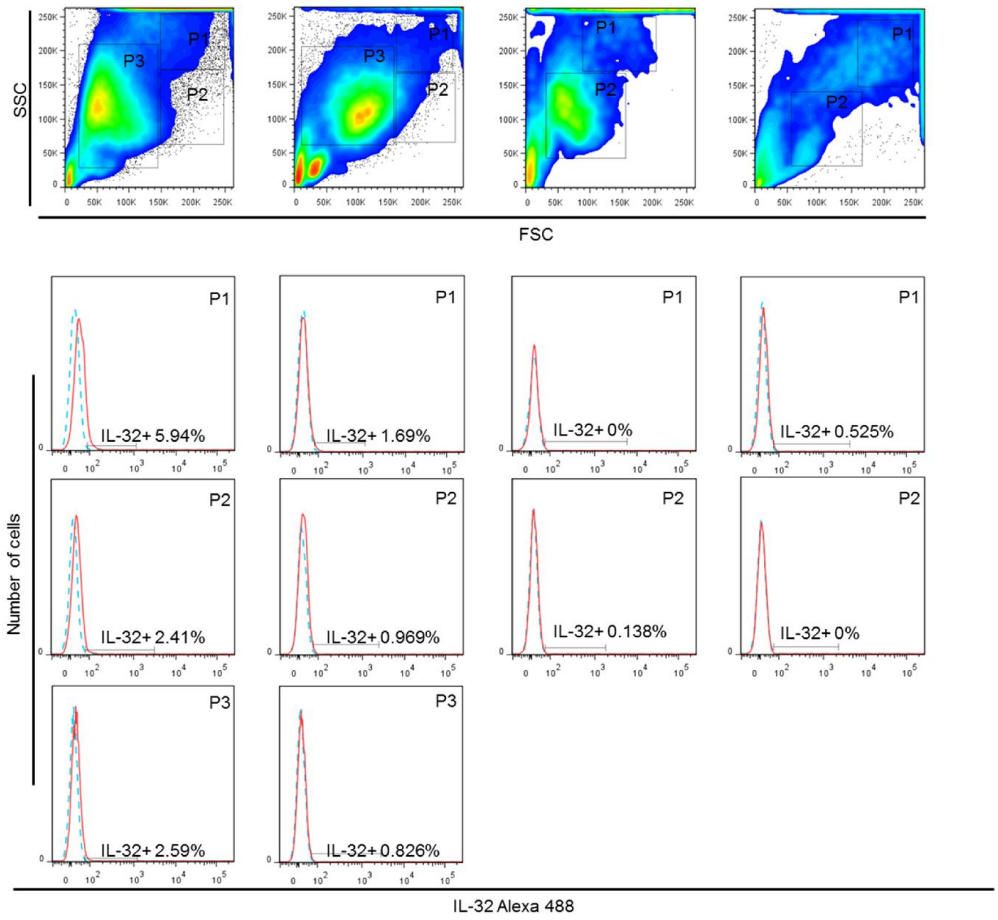

Figure 4.13 Selective gating for identification of IL-32 expression cells in myeloma CD138$^+$ enriched plasma cells.
Enriched CD138$^+$ plasma cells were fixed and stained for intra-cellular IL-32 with anti-IL32 or isotype control, and analyzed by LSR II flow cytometer. Dot plots of distinct subpopulation of CD138$^+$ plasma cells with different FSC/SSC patterns (upper panels). The histograms of IL-32 staining of the gated populations (lower panels). The percentage indicated IL-32$^+$ cells of the gated subpopulation of CD138$^+$ plasma cells (lower panels). (n=4) Isotype control was used as a negative control (dotted blue line).

Table 4.4 Percentage of IL-32$^+$ cells in total and selective gated cells

Patient ID	IL-32+ cells (%)			
	Total gated	Sub population P1	Sub population P2	Sub population P3
1675	1.98	5.94	2.41	2.59
1714	0.79	1.69	0.969	0.826
1716	0.227	0	0.138	-
1122	0.23	0.525	0	-

4.2.5. C. Phenotype of IL-32 producing CD138$^+$ plasma cells

Myeloma cells are generally identified by Flow cytometry as CD19$^-$, CD38^{high} (as well as by the presence of either kappa or lambda immunoglobulin light chain to determine clonality) [88]. Although many myeloma cells express CD138 and are normally CD45$^-$, both CD138 and CD45 expression on plasma cells can vary between patients [88]. In an attempt to identify which plasma cells express IL-32, enriched CD138$^+$ plasma cells were surface stained with surface markers against CD38 and CD45 before the intracellular staining as described in materials and methods and analyzed by Flow cytometry. In this experiment gates were set on live cells (with FSC versus SSC). Then, the gated population was checked for IL-32 expression. The isotype control was used as a negative control to set the histogram and dot plot gates (Appendix III). Histogram plot showing the percentage of IL-32$^+$ population is indicated in Figure 4.14. In addition a dot plot of CD38 and CD45 staining of the IL-32$^+$ cells is shown (Figure 4.14 lower panels). We could detect only a small number of IL-32 expressing cells in this patient (donor 5) as only 4.77% IL-32$^+$ cells were found in the enriched CD138$^+$ fraction. This is shown in the histogram plot (Figure 4.14 upper right panel). These IL-32$^+$ cells expressed CD38 but not CD45.

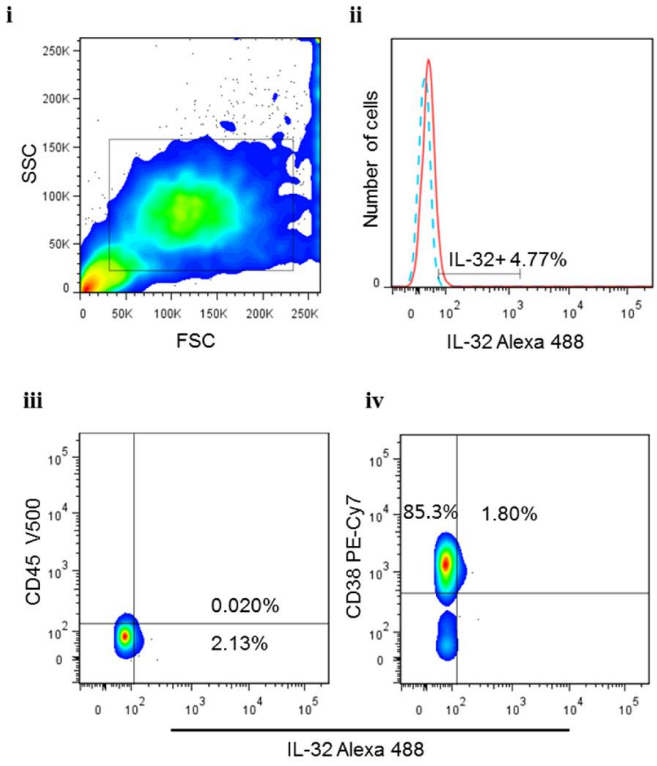

Figure 4.14 Phenotype of IL-32 expressing cells in CD138$^+$ fraction.
Enriched CD138$^+$ fraction was surface stained with antibodies against CD38 and CD45 markers, fixed and then subjected to intra-cellular staining for IL-32 before analysis on LSR II Flow cytometer. Gated cells with FSC versus SSC (i). Histogram plot of IL-32 staining of the gated population (ii). The percentage indicated IL-32$^+$ cells of the gated population (ii). Dot plot of CD45 profile of the IL-32$^+$ cells (iii). Dot plot of CD38 profile of the IL-32$^+$ cells (iv). Isotype control was used as a negative control (dotted blue line).

4.2.6 Identification of IL-32 expressing cells within CD138$^-$ bone marrow populations

IL-32 was found in the bone marrow plasma cells. The source of IL-32 could be myeloma cells, but it could also be secreted from other cell types within the bone marrow such as T cells and monocytes, which are known to produce IL-32 in inflammatory conditions [89]. Natural killer cells (NK) are also a well-known source of IL-32 [90]. As we described earlier, there are different cell types in the bone microenvironment such as B cells, T cells and monocytes. Monocytes at least are well characterized players in myeloma disease progression and bone destruction [91]. We therefore asked whether the different immune cells would express IL-32 in the bone marrow of myeloma patients. For this experiment we used CD138$^-$ fraction, after enrichment of the CD138$^+$ cells from bone marrow mononuclear cells. These cells were stained in a 4-color flow cytometric assay with antibodies against T cells, B cells and monocytes as well as IL-32 as described in materials and methods. The isotype control was used as a negative control to set the histogram and dot plot gates (Appendix IV). We could detect a minor population of IL-32 expressing cells in this patient (donor 1819) as 8.11% cells are positive for IL-32, as indicated in the histogram plot (Figure 4.15 upper right panel). We also observed a small proportion of IL-32$^+$ cells within CD3$^+$ T cell and CD14$^+$ monocyte fractions as 2.59% and 1.98% respectively are positive for IL-32 as shown in dot plots (Figure 4.15 lower panels) while IL-32 was not expressed on CD19$^+$ B cells.

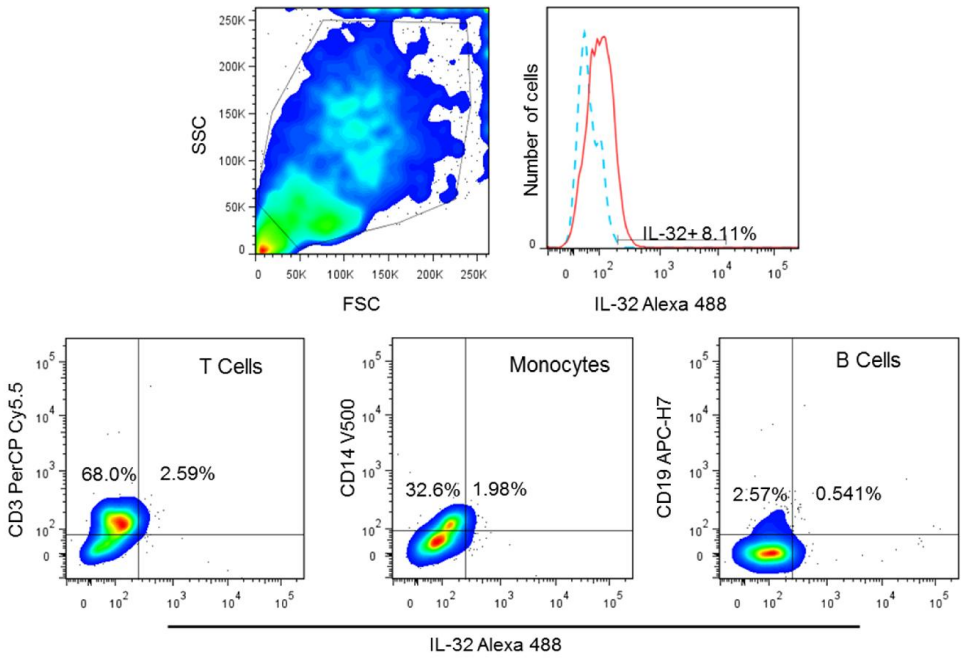

Figure 4.15 IL-32 expression in the myeloma bone marrow CD138$^-$ fraction
CD138$^-$ fraction was surface stained with antibodies against CD3, CD14, CD19, fixed and then subjected to intracellular staining for IL-32 before analysis on LSR II Flow cytometer. The gate was set on live cells with FSC versus SSC (upper panel). Histogram plot showing IL-32 staining of one patient (upper panel). Percentage of IL-32$^+$ cells of the gated cells (upper panel). Dot plots of CD3, CD14 and CD19 staining of the IL-32$^+$ cells (lower panels). Gates indicated IL-32$^+$ cells (left panels). The isotype control was used as a negative control (Dotted blue line).

4. 3 Summary IL-32 staining

Collectively our flow analysis indicated that myeloma cell lines JJN3 and H929 expressed intracellular IL-32. In contrast, we found none or very few intracellular IL-32^+ cells in the $CD138^+$ fraction from these 4 myeloma patients. It was also observed that some plasma cells within the bone marrow of one myeloma patient expressed IL-32 and others did not. We found that a small proportion of malignant cells identified as $CD138^+$ $CD38^+$ and $CD45^-$ from one patient expressed IL-32. In addition in the only one patient analyzed, we found a small number of IL-32^+ cells. In addition, we could only show one patient expressing a small proportion of IL-32^+ cells within the $CD138^-$ fraction. These accounted for a minor population of $CD3^+$ T cells and $CD14^+$ monocytes.

5. Discussion

5.1 RANK expression on marrow myeloid cells in myeloma patients

Tumor inducing osteoclasts differentiation and activation that lead to defective bone remodeling is a common feature seen in many types of cancers including MM, breast, lung and prostate cancers. However, myeloma is unique among malignancies in its propensity to cause extensive bone destruction. Increased bone loss is due to increased number and activity osteoclasts bone resorbing cells. This is at least in part, caused by persistently increased levels of RANKL production from myeloma cells and other bone cells, enhancing bone resorption through the classical RANK/RANKL pathway. Osteoclast precursors are poorly characterized in myeloma as well as in other inflammatory conditions like psoriatic arthritis essentially due to fact that it is not clear from which cells osteoclasts originate and it is not yet firmly established which surface markers these precursor cells express. From the literature we know that RANK is expressed on osteoclast precursors, as well as on mature osteoclasts and that its function is necessary for osteoclastogenesis [84, 92].

We used flow cytometric analysis to study the RANK expression on $CD14^+$ monocytes and on $CD66b^+$ granulocytes in the bone marrow aspirates obtained from 14 patients with MGUS and multiple myeloma. Lineage cells CD3 and CD19 (B cells and T cells) present in the bone marrow were not labeled with anti-RANK antibodies.

We showed that RANK was detectable on the surface of human monocytic cell line THP-1 after stimulation with M-CSF. This is in line with a previous report by Arai Fumio et al., (1999) who demonstrated that RANK expression on early osteoclast precursors cells is up-regulated after stimulation with M-CSF [84]. We found in this study that the proportion of $RANK^+$ cells varied among the myeloma patients. RANK was found at low frequency on $CD14^+$ monocytes in the bone marrow as only two patients (2/14) had high and intermediate proportions of $RANK^+$ cells. We also found significantly fewer $RANK^+$ granulocytes than $RANK^+$ monocytes in the bone marrow of myeloma patients. In addition, our findings indicated that there are very few $RANK^+$ granulocytes and monocytes even in the patients with high tumor load (> 60% PCs).

Several *in vitro* studies used human PBMCs or purified $CD14^+$ PBMNCs [51] to generate mature and active osteoclasts. Other relevant studies reported that $CD14^+$ bone marrow monocytes were $RANK^+$ and therefore a reliable source of committed pre-OCs [51]. In line with the assumption that osteoclast precursors are largely formed from myeloid precursors that belong to the monocyte lineage, we found significantly fewer $RANK^+$ granulocytes than $RANK^+$ monocytes in the bone marrow of myeloma patients. None or very few $RANK^+$ granulocytes were detected even in the patients that had a high RANK expression on their monocytes (2/14). A recent study observed increased RANK expression in uncultured, undifferentiated (M-CSF only) myeloma patient's bone marrow monocytes compared that

from normal donors. Interestingly, the study also reported that the level of RANK protein was increased only in 3 out of 11 myeloma patients compared to normal donor in BMM cultures [91]. In addition, Atkins and colleagues (2016) showed high percentage of $CD14^+$ monocytes expressing RANK [81]. Similar to these studies, our data showed that $CD14^+$ monocytes had more $RANK^+$ cells than granulocytes (see Table 4.1), although only a few of the myeloma patients (2/14) had high proportions of $RANK^+$ monocytes. Therefore, this supports our findings that only a few of our patients had $RANK^+$ monocytes. There were however, more $RANK^+$ $CD14^+$ monocytes than granulocytes. It should be noted that RANK is not only confined to monocytes, as other cells in the bone compartment can also express RANK. For example myeloid derived dendritic cells [93], $CD3^+$ T cells in the bone marrow, are in addition to monocytes positive for RANK expression [81, 86]. RANK expression was also observed in mononuclear cells with the morphology of erythroblasts in the bone marrow of myeloma patients [94]. Thus it may be possible that other bone marrow cells which express RANK could differentiate into osteoclasts and this could explain our findings. If there are more $RANK^+$ monocytes in the bone marrow than blood, contamination with peripheral blood during sample collection could also explain, why only few patients have $RANK^+$ monocytes. Alternatively, RANK could be expressed on subpopulations of monocytes. Monocytes are heterogeneous and can for example be subdivided into subpopulations based on CD14 and CD16 surface markers [95]. A minor subpopulation which is $CD14^{dim}$ and $CD16^+$, namely non-classical monocytes [96], was found to be implicated in inflammatory conditions and cancer [97, 98]. Recently, our group observed higher proportions of $CD16^+$ $CD14^{dim}$ monocytes in the bone marrow of myeloma patients with high tumor load compared with those with low tumor load [99]. Interestingly, Chiu et al., (2010) showed that monocytes cultured in the presence of M-CSF and RANKL up-regulated CD16 expression [100]. Moreover, increased in osteoclast precursors was recently proposed to reside in the $CD14^{low}$ $CD16^+$ monocytes fraction in patients with psoriatic arthritis, particularly those with bone erosions [101]. Therefore one might speculate whether other monocyte subsets such as the non-classical monocytes could be osteoclast precursors and the low expression of CD14 on these cells could explain why few $RANK^+$ cells were present in the monocyte fraction.

5.1.1 RANK expression on granulocytes

We found no or very few $CD66^+$ $RANK^+$ granulocytes in the myeloma patients. Granulocytes, originating in the bone marrow environment are found to store their cytotoxic content of enzymes and receptors in secretory vesicles and granules [102]. Recent literature reported that RANK is exported to the surface of a granulocytes population following stimulation *in vitro* and increasing the level of Ca^{2+}. RANK was also found be up-regulated on $CD66b^+$ granulocytes in patients with persistent bacterial infections [82]. These data suggested that the RANK expression is strongly modulated and it require

activation in order to mobilize their intracellular components to the cell membrane. Alexander and collogues., (2012) also showed that RANK was up-regulated in the peripheral blood as a result of activation indicating that local factors released in the periphery or within the inflamed area and during persistent infections are important [82]. Similarly granulocytic cells from the inflamed synovial tissue of patients with RA expressed RANK [103]. Because myeloma patients have a high risk of developing infections [104], patients recruited in these studies may have also such complications. Therefore, it would be interesting to see if the RANK expression is increased in circulating granulocytes and whether or not RANK expression on granulocytes correlate with the presence of infections in myeloma patients. However, there are reports that RANK is not only up-regulated during infections or inflammatory conditions. For example, RANK expression on $CD66b^+$ granulocytes varied in healthy humans ranging from less than 1% to 70% [76]. It could be that our myeloma patients fell into the lower ranges of RANK expression expressed by granulocytes.

5.1.2 RANK expression in myeloma patients with high tumor load

Literature suggested a clear association between patient's tumor load, osteoclast number, and osteoclast resorbtive area in the bone marrow biopsies from MM patients [105]. However, our data showed that the majority of patients (5/14) had very low numbers or no $RANK^+$ monocytes and granulocytes in the bone even though they had high tumor load and concomitant presence of bone lesions. This could suggest that there may be not many osteoclast precursors needed to develop into active bone resorbing osteoclasts. One explanation could be that factors released by tumor cells are important in supporting osteoclast formation in the bone environment, independently of the number of osteoclast precursors. A similar mechanism is seen in breast cancer patients where the increased bone resorption process is not due to an increase number of osteoclast precursors but rather factors that are released at tumor site are important in promoting osteoclasts differentiation and activity [106].

In addition to early osteoclast precursors, RANK is also a feature of the mature osteoclast. It has been reported that mature osteoclasts are derived predominantly from $CD14^+$ monocytes which lose CD14 marker during the later stages of osteoclast differentiation [51]. Thus the low frequency of RANK expressing monocytes in the patients with high tumor load and lytic lesions could be because the proportion of $RANK^+$ cells within the $CD14^+$ monocyte fraction will drop as the $RANK^+$ precursor has matured into functionally active osteoclast [51]. This suggests that RANK might be up-regulated only in early stages of osteoclast development and is important for lineage commitment, but probably not required for the specialized function of bone resorption and is therefore not expressed at this stage [51]. Alternative explanation to our findings can be also that $RANK^+$ monocytes have already differentiated into bone resorbing cells, lodged in the bone and therefore not seen in the aspirate in our patients with bone disease.

5.2 IL-32 expression in the bone marrow cells in myeloma patients

IL-32 has gained attention as a pro-inflammatory cytokine, that can promote differentiation of innate immune cells like human blood monocytes [66] and stimulate cells to produce inflammatory cytokines. It is also highly expressed by several other immune and non-immune cells such as activated T cells, NK-cells and epithelial cells [63].

It plays a key role in several pathological conditions such as cancer and is elevated in various human tissue and several inflammatory diseases such as inflammatory bowel disease (IBD) [107] and rheumatoid arthritis [68]. This suggests that it may also be involved in myeloma pathogenesis.

Our research group found that IL-32 was highly expressed in primary myeloma cells and cell lines when measured at the mRNA level. In addition, it was found be secreted into the supernatant of myeloma cell lines and in bone marrow plasma of myeloma patients. Confocal data confirmed the presence of intracellular IL-32 in myeloma cell lines JJN3 and H929 (Zahoor and Standal, manuscript in preparation). However, our flow analysis for IL-32 showed that intra-cellular IL-32 was detected only in myeloma cell lines and not in the patients, as very few IL-32^{+} plasma cells were found in the bone marrow. The discrepancy between high mRNA and low protein in primary myeloma cells could suggest that either IL-32 is tightly regulated translational or post-translationally or is expressed by a small proportion of plasma cells in the myeloma patients as suggested by our results from the selective gating. IL-32 is secreted from the plasma cells and may therefore not be efficiently detected in the cytoplasm. Therefore letting it accumulate within the cells by treating them with brefeldin A or monensin, that prevents protein transport from Endoplasmic reticulum (ER) to Golgi complex and secreting vesicles, could allow its detection. This method is routinely used to detect intracellular cytokines in activated T cells.

Alternatively, IL-32 secretion could be directly stimulated by cell-cell interaction within the bone marrow or by factors present in the local micro-environment, known to stimulate the release of different cytokines [32]. It might be possible that IL-32 is transcribed and synthesized, followed by storage in secretary granules and then released upon stimulation by signals from micro-environment, similar to insulin-secretion pathway by exocytosis followed by high level of intracellular glucose and calcium [108]. Primary myeloma cells in its own micro-environment may have a continuous stimulation from other cells which induce a constant synthesis and secretion of IL-32, thus removing the cells from bone marrow environment could cease the secretion of IL-32 in the primary cells. To address this question, one approach for detection of IL-32 by flow cytometry would be to culture primary cells without bone marrow stromal cells from myeloma patients and see if the absence of stimuli from micro-environment results in an increase of IL-32 intra-cellular accumulation.

5.3 Study limitations and challenges

We received fresh bone marrow aspirate from patients as they came to the clinic or it was mailed to the laboratory from clinics around Norway. Thus, the patient material sometimes arrived at infrequent intervals. Therefore, in the limited time frame available did not allow us to perform our analysis on statistically acceptable sample sizes to be able to draw a final conclusion. Additionally, detailed disease history, diagnosis and clinical parameters were not yet available at the time of writing. As the information about patients from outside of Trondheim is often a challenging and time consuming task. Therefore, to establish a reliable correlation of experimental results and disease manifestation more patients and better clinical data are necessary.

We observed, that while some cell lines expressed IL-32, only a very few of the primary cells expressed IL-32. It is possible that IL-32 was secreted. In future experiments it would be considered to inhibit protein transport by using Brefeldin A. that is very often used in intracellular staining procedure to enable detection of secreted cytokines. The identification and characterization of IL-32 expressing $CD138^{+}$ cells would also be required and might lead to important findings about its role in myeloma progression. Obtaining more patient's bone marrow samples and disease history/clinical diagnosis was also an obstacle in IL-32 study. IL-32 expression and its correlation with different parameters of disease activity such as M-protein serum levels, % of plasma cells and presence of bone lesion could also be important in this study. Therefore, we proposed to include a larger cohort of myeloma patients.

6 Conclusions and future perspectives

Osteolytic lesions are crucial events in disease manifestation of multiple myeloma that not only cause sever bone pain but also aggravate tumor growth. RANKL-RANK signaling provides base line for generating bone eroding osteoclasts. RANKL-RANK signaling not only plays a major role in osteoclasts differentiation but also define the fate of osteoclast precursor cells. Despite the established role of osteoclastogenesis in Multiple myeloma and other bone diseases, the detailed identity of osteoclast precursors remains unknown. Therefore, we set out to investigate, if bone marrow granulocytes could be potential osteoclast precursors in multiple myeloma patients.

We determined the abundance of $RANK^+$ on granulocytes in the bone marrow aspirates from myeloma patients and our results from 14 patients showed that very few $RANK^+$ granulocytes were detected in the bone marrow aspirates of these myeloma patients, even in the patients that had a lot of monocytes expressing RANK. These might suggest that monocytes are primed source of osteoclast precursors. However further studies with more patients are required, as well as including healthy controls to get a clear picture of osteoclast precursor phenotype in Multiple myeloma.

In the next project, we were interested in evaluating the status of IL-32 expression in myeloma patient's bone marrow cells. We only managed to test a few myeloma patients and in this very small cohort, few IL-32 expressing cells were observed in the enriched $CD138^+$ fraction and as well as in the other bone marrow cells that did not express CD138. When we looked at the cells with different scatter properties within the $CD138^+$ population, our results indicated that a subpopulation of $CD138^+$ plasma cells expressed IL-32. In the $CD138^-$ fraction, a small population of T-cells and monocytes were expressing IL-32. However, further details about the phenotype of these cells are required to identify the IL-32 expressing cells, in both fractions. We therefore propose that IL-32 is secreted by a small proportion of plasma cells. An alternative explanation to this could be that cytokine are rapidly secreted and therefore not detectable in the cytoplasm of the primary plasma cells. The fact that IL-32 is found in the bone marrow plasma, suggest that this might be the case.

7 References

1. Kvam, A.K. and A. Waage, *Health-related quality of life in patients with multiple myeloma - does it matter?* Haematologica, 2015. **100**(6): p. 704-705.
2. Kyle, R.A., et al., *Review of 1027 patients with newly diagnosed multiple myeloma.* Mayo Clin Proc, 2003. **78**(1): p. 21-33.
3. Hideshima, T., et al., *Understanding multiple myeloma pathogenesis in the bone marrow to identify new therapeutic targets.* Nat Rev Cancer, 2007. **7**(8): p. 585-98.
4. Roodman, G.D., *Pathogenesis of myeloma bone disease.* J Cell Biochem, 2010. **109**(2): p. 283-91.
5. Edwards, C.M., J. Zhuang, and G.R. Mundy, *The pathogenesis of the bone disease of multiple myeloma.* Bone. **42**(6): p. 1007-1013.
6. Ludwig, H., et al., *Survival and years of life lost in different age cohorts of patients with multiple myeloma.* J Clin Oncol, 2010. **28**(9): p. 1599-605.
7. Alexander, D.D., et al., *Multiple myeloma: a review of the epidemiologic literature.* Int J Cancer, 2007. **120 Suppl 12**: p. 40-61.
8. Becker, N., *Epidemiology of multiple myeloma.* Recent Results Cancer Res, 2011. **183**: p. 25-35.
9. Siegel, R., D. Naishadham, and A. Jemal, *Cancer statistics, 2012.* CA Cancer J Clin, 2012. **62**(1): p. 10-29.
10. Waxman, A.J., et al., *Racial disparities in incidence and outcome in multiple myeloma: a population-based study.* Blood, 2010. **116**(25): p. 5501-6.
11. Raab, M.S., et al., *Multiple myeloma.* The Lancet. **374**(9686): p. 324-339.
12. Prideaux, S.M., E. Conway O'Brien, and T.J. Chevassut, *The genetic architecture of multiple myeloma.* Adv Hematol, 2014. **2014**: p. 864058.
13. Kyle, R.A. and S.V. Rajkumar, *Criteria for diagnosis, staging, risk stratification and response assessment of multiple myeloma.* Leukemia, 2009. **23**(1): p. 3-9.
14. Pratt, G., *Molecular aspects of multiple myeloma.* Mol Pathol, 2002. **55**(5): p. 273-83.
15. Bianchi, G. and N.C. Munshi, *Pathogenesis beyond the cancer clone(s) in multiple myeloma.* Blood, 2015. **125**(20): p. 3049-58.
16. Attaelmannan, M. and S.S. Levinson, *Understanding and identifying monoclonal gammopathies.* Clin Chem, 2000. **46**(8 Pt 2): p. 1230-8.
17. Palumbo, A. and K. Anderson, *Multiple myeloma.* N Engl J Med, 2011. **364**(11): p. 1046-60.
18. Shapiro-Shelef, M. and K. Calame, *Regulation of plasma-cell development.* Nat Rev Immunol, 2005. **5**(3): p. 230-42.

19. Halliley, J.L., et al., *Long-Lived Plasma Cells Are Contained within the CD19(-)CD38(hi)CD138(+) Subset in Human Bone Marrow.* Immunity, 2015. **43**(1): p. 132-45.
20. Raja, K.R., L. Kovarova, and R. Hajek, *Review of phenotypic markers used in flow cytometric analysis of MGUS and MM, and applicability of flow cytometry in other plasma cell disorders.* Br J Haematol, 2010. **149**(3): p. 334-51.
21. Kuehl, W.M. and P.L. Bergsagel, *Molecular pathogenesis of multiple myeloma and its premalignant precursor.* J Clin Invest, 2012. **122**(10): p. 3456-63.
22. Morgan, G.J., B.A. Walker, and F.E. Davies, *The genetic architecture of multiple myeloma.* Nat Rev Cancer, 2012. **12**(5): p. 335-348.
23. Morgan, G.J., B.A. Walker, and F.E. Davies, *The genetic architecture of multiple myeloma.* Nat Rev Cancer, 2012. **12**(5): p. 335-48.
24. Yaccoby, S., et al., *Cancer and the microenvironment: myeloma-osteoclast interactions as a model.* Cancer Res, 2004. **64**(6): p. 2016-23.
25. Raje, N. and G.D. Roodman, *Advances in the biology and treatment of bone disease in multiple myeloma.* Clin Cancer Res, 2011. **17**(6): p. 1278-86.
26. Manier, S., et al., *Bone marrow microenvironment in multiple myeloma progression.* J Biomed Biotechnol, 2012. **2012**: p. 157496.
27. Danks, L. and H. Takayanagi, *Immunology and bone.* Journal of Biochemistry, 2013. **154**(1): p. 29-39.
28. Balakumaran, A., et al., *Bone marrow microenvironment in myelomagenesis: its potential role in early diagnosis.* Expert Rev Mol Diagn, 2010. **10**(4): p. 465-80.
29. Basak, G.W., et al., *Multiple myeloma bone marrow niche.* Curr Pharm Biotechnol, 2009. **10**(3): p. 345-6.
30. Fowler, J.A., C.M. Edwards, and P.I. Croucher, *Tumor-host cell interactions in the bone disease of myeloma.* Bone, 2011. **48**(1): p. 121-8.
31. Oranger, A., et al., *Cellular Mechanisms of Multiple Myeloma Bone Disease.* Clinical and Developmental Immunology, 2013. **2013**: p. 11.
32. Silvestris, F., et al., *Bone-resorbing cells in multiple myeloma: osteoclasts, myeloma cell polykaryons, or both?* Oncologist, 2009. **14**(3): p. 264-75.
33. Hideshima, T., et al., *Advances in biology of multiple myeloma: clinical applications.* Blood, 2004. **104**(3): p. 607-18.
34. Sanderson, R.D. and Y. Yang, *Syndecan-1: a dynamic regulator of the myeloma microenvironment.* Clin Exp Metastasis, 2008. **25**(2): p. 149-59.
35. Standal, T., et al., *Osteoprotegerin is bound, internalized, and degraded by multiple myeloma cells.* Blood, 2002. **100**(8): p. 3002-7.

36. Yang, Y., et al., *Heparanase enhances syndecan-1 shedding: a novel mechanism for stimulation of tumor growth and metastasis.* J Biol Chem, 2007. **282**(18): p. 13326-33.
37. Hameed, A., et al., *Bone disease in multiple myeloma: pathophysiology and management.* Cancer Growth Metastasis, 2014. **7**: p. 33-42.
38. Anderson, D.M., et al., *A homologue of the TNF receptor and its ligand enhance T-cell growth and dendritic-cell function.* Nature, 1997. **390**(6656): p. 175-9.
39. Mainwaring, C.J., et al., *Monocyte dysfunction in patients with multiple myeloma and lymphoplasmacytic disorders is related to serum paraprotein levels.* Br J Haematol, 1999. **105**(4): p. 948-54.
40. Edwards, C.M., J. Zhuang, and G.R. Mundy, *The pathogenesis of the bone disease of multiple myeloma.* Bone, 2008. **42**(6): p. 1007-13.
41. Pearse, R.N., et al., *Multiple myeloma disrupts the TRANCE/ osteoprotegerin cytokine axis to trigger bone destruction and promote tumor progression.* Proc Natl Acad Sci U S A, 2001. **98**(20): p. 11581-6.
42. Silbermann, R. and G.D. Roodman, *Myeloma bone disease: Pathophysiology and management.* J Bone Oncol, 2013. **2**(2): p. 59-69.
43. Tian, E., et al., *The role of the Wnt-signaling antagonist DKK1 in the development of osteolytic lesions in multiple myeloma.* N Engl J Med, 2003. **349**(26): p. 2483-94.
44. Romano, A., et al., *Immunological Dysregulation in Multiple Myeloma Microenvironment.* Biomed Research International, 2014.
45. Tanaka, Y., et al., *Myeloma cell-osteoclast interaction enhances angiogenesis together with bone resorption: a role for vascular endothelial cell growth factor and osteopontin.* Clin Cancer Res, 2007. **13**(3): p. 816-23.
46. Abe, M., et al., *Osteoclasts enhance myeloma cell growth and survival via cell-cell contact: a vicious cycle between bone destruction and myeloma expansion.* Blood, 2004. **104**(8): p. 2484-91.
47. Redzepovic, J., et al., *Current trends in multiple myeloma management.* J Int Med Res, 2008. **36**(3): p. 371-86.
48. Roodman, G.D., *Pathogenesis of myeloma bone disease.* Leukemia, 2009. **23**(3): p. 435-41.
49. Soysa, N.S., et al., *Osteoclast formation and differentiation: an overview.* J Med Dent Sci, 2012. **59**(3): p. 65-74.
50. Xiao, Y., et al., *Identification of the Common Origins of Osteoclasts, Macrophages, and Dendritic Cells in Human Hematopoiesis.* Stem Cell Reports, 2015. **4**(6): p. 984-94.
51. Massey, H.M. and A.M. Flanagan, *Human osteoclasts derive from CD14-positive monocytes.* Br J Haematol, 1999. **106**(1): p. 167-70.

52. Simonet, W.S., et al., *Osteoprotegerin: a novel secreted protein involved in the regulation of bone density.* Cell, 1997. **89**(2): p. 309-19.

53. Hsu, H., et al., *Tumor necrosis factor receptor family member RANK mediates osteoclast differentiation and activation induced by osteoprotegerin ligand.* Proc Natl Acad Sci U S A, 1999. **96**(7): p. 3540-5.

54. Boyle, W.J., W.S. Simonet, and D.L. Lacey, *Osteoclast differentiation and activation.* Nature, 2003. **423**(6937): p. 337-342.

55. Adamopoulos, I.E. and E.D. Mellins, *Alternative pathways of osteoclastogenesis in inflammatory arthritis.* Nat Rev Rheumatol, 2015. **11**(3): p. 189-194.

56. Yasuda, H., et al., *Identity of osteoclastogenesis inhibitory factor (OCIF) and osteoprotegerin (OPG): a mechanism by which OPG/OCIF inhibits osteoclastogenesis in vitro.* Endocrinology, 1998. **139**(3): p. 1329-37.

57. Suda, T., et al., *Modulation of osteoclast differentiation and function by the new members of the tumor necrosis factor receptor and ligand families.* Endocr Rev, 1999. **20**(3): p. 345-57.

58. Dai, X.M., et al., *Targeted disruption of the mouse colony-stimulating factor 1 receptor gene results in osteopetrosis, mononuclear phagocyte deficiency, increased primitive progenitor cell frequencies, and reproductive defects.* Blood, 2002. **99**(1): p. 111-20.

59. Shalhoub, V., et al., *Characterization of osteoclast precursors in human blood.* Br J Haematol, 2000. **111**(2): p. 501-12.

60. Atkins, G.J., et al., *RANK Expression as a cell surface marker of human osteoclast precursors in peripheral blood, bone marrow, and giant cell tumors of bone.* J Bone Miner Res, 2006. **21**(9): p. 1339-49.

61. Wakkach, A., et al., *Bone marrow microenvironment controls the in vivo differentiation of murine dendritic cells into osteoclasts.* Blood, 2008. **112**(13): p. 5074-83.

62. Tucci, M., et al., *Immature dendritic cells in multiple myeloma are prone to osteoclast-like differentiation through interleukin-17A stimulation.* Br J Haematol, 2013. **161**(6): p. 821-31.

63. Dahl, C.A., et al., *Identification of a novel gene expressed in activated natural killer cells and T cells.* J Immunol, 1992. **148**(2): p. 597-603.

64. Kim, S.H., et al., *Interleukin-32: a cytokine and inducer of TNFalpha.* Immunity, 2005. **22**(1): p. 131-42.

65. Netea, M.G., et al., *IL-32 synergizes with nucleotide oligomerization domain (NOD) 1 and NOD2 ligands for IL-1beta and IL-6 production through a caspase 1-dependent mechanism.* Proc Natl Acad Sci U S A, 2005. **102**(45): p. 16309-14.

66. Netea, M.G., et al., *Interleukin-32 induces the differentiation of monocytes into macrophage-like cells.* Proc Natl Acad Sci U S A, 2008. **105**(9): p. 3515-20.

67. Kim, Y.G., et al., *Effect of interleukin-32gamma on differentiation of osteoclasts from CD14+ monocytes.* Arthritis Rheum, 2010. **62**(2): p. 515-23.

68. Joosten, L.A., et al., *IL-32, a proinflammatory cytokine in rheumatoid arthritis.* Proc Natl Acad Sci U S A, 2006. **103**(9): p. 3298-303.

69. Xu, W.D., et al., *IL-32 with potential insights into rheumatoid arthritis.* Clin Immunol, 2013. **147**(2): p. 89-94.

70. Tsai, C.Y., et al., *Interleukin-32 increases human gastric cancer cell invasion associated with tumor progression and metastasis.* Clin Cancer Res, 2014. **20**(9): p. 2276-88.

71. Nold, M.F., et al., *Endogenous IL-32 controls cytokine and HIV-1 production.* J Immunol, 2008. **181**(1): p. 557-65.

72. Bai, X., et al., *Human IL-32 expression protects mice against a hypervirulent strain of Mycobacterium tuberculosis.* Proc Natl Acad Sci U S A, 2015. **112**(16): p. 5111-6.

73. Marcondes, A.M., et al., *Dysregulation of IL-32 in myelodysplastic syndrome and chronic myelomonocytic leukemia modulates apoptosis and impairs NK function.* Proc Natl Acad Sci U S A, 2008. **105**(8): p. 2865-70.

74. Dinarello, C.A. and S.H. Kim, *IL-32, a novel cytokine with a possible role in disease.* Ann Rheum Dis, 2006. **65 Suppl 3**: p. iii61-4.

75. Joosten, L.A., et al., *Novel insights into the biology of interleukin-32.* Cell Mol Life Sci, 2013. **70**(20): p. 3883-92.

76. Riegel, A., et al., *Human polymorphonuclear neutrophils express RANK and are activated by its ligand, RANKL.* Eur J Immunol, 2012. **42**(4): p. 975-81.

77. Kim, C.W., et al., *Members of the syndecan family of heparan sulfate proteoglycans are expressed in distinct cell-, tissue-, and development-specific patterns.* Mol Biol Cell, 1994. **5**(7): p. 797-805.

78. Sanderson, R.D., P. Lalor, and M. Bernfield, *B lymphocytes express and lose syndecan at specific stages of differentiation.* Cell Regul, 1989. **1**(1): p. 27-35.

79. Maecker, H.T. and J. Trotter, *Flow cytometry controls, instrument setup, and the determination of positivity.* Cytometry A, 2006. **69**(9): p. 1037-42.

80. Petitprez, V., et al., *CD14+CD16+ monocytes rather than CD14+CD51/61+ monocytes are a potential cytological marker of circulating osteoclast precursors in multiple myeloma. A preliminary study.* International Journal of Laboratory Hematology, 2015. **37**(1): p. 29-35.

81. Atkins, G.J., et al., *RANK expression as a cell surface marker of human osteoclast precursors in peripheral blood, bone marrow, and giant cell tumors of bone.* Journal of Bone and Mineral Research, 2006. **21**(9): p. 1339-1349.

82. Riegel, A., et al., *Human polymorphonuclear neutrophils express RANK and are activated by its ligand, RANKL.* European Journal of Immunology, 2012. **42**(4): p. 975-981.

83. Park, K.Y., W.A. Li, and M.O. Platt, *Patient specific proteolytic activity of monocyte-derived macrophages and osteoclasts predicted with temporal kinase activation states during differentiation.* Integr Biol (Camb), 2012. **4**(12): p. 1459-69.

84. Arai, F., et al., *Commitment and differentiation of osteoclast precursor cells by the sequential expression of c-Fms and receptor activator of nuclear factor kappaB (RANK) receptors.* J Exp Med, 1999. **190**(12): p. 1741-54.

85. Wei, A. and S. Juneja, *Bone marrow immunohistology of plasma cell neoplasms.* J Clin Pathol, 2003. **56**(6): p. 406-11.

86. Kotani, M., et al., *Systemic circulation and bone recruitment of osteoclast precursors tracked by using fluorescent imaging techniques.* J Immunol, 2013. **190**(2): p. 605-12.

87. Robillard, N., et al., *Immunophenotype of normal and myelomatous plasma-cell subsets.* Front Immunol, 2014. **5**: p. 137.

88. Kumar, S., T. Kimlinger, and W. Morice, *Immunophenotyping in multiple myeloma and related plasma cell disorders.* Best Pract Res Clin Haematol, 2010. **23**(3): p. 433-51.

89. Mabilleau, G. and A. Sabokbar, *Interleukin-32 promotes osteoclast differentiation but not osteoclast activation.* PLoS One, 2009. **4**(1): p. e4173.

90. Goda, C., et al., *Involvement of IL-32 in activation-induced cell death in T cells.* Int Immunol, 2006. **18**(2): p. 233-40.

91. Cao, H., et al., *Critical role of AKT protein in myeloma-induced osteoclast formation and osteolysis.* J Biol Chem, 2013. **288**(42): p. 30399-410.

92. Nakagawa, N., et al., *RANK is the essential signaling receptor for osteoclast differentiation factor in osteoclastogenesis.* Biochem Biophys Res Commun, 1998. **253**(2): p. 395-400.

93. Anderson, D.M., et al., *A homologue of the TNF receptor and its ligand enhance T-cell growth and dendritic-cell function.* Nature, 1997. **390**(6656): p. 175-179.

94. Roux, S. and X. Mariette, *The high rate of bone resorption in multiple myeloma is due to RANK (receptor activator of nuclear factor-kappaB) and RANK Ligand expression.* Leuk Lymphoma, 2004. **45**(6): p. 1111-8.

95. Passlick, B., D. Flieger, and H.W. Ziegler-Heitbrock, *Identification and characterization of a novel monocyte subpopulation in human peripheral blood.* Blood, 1989. **74**(7): p. 2527-34.

96. Tallone, T., et al., *Heterogeneity of human monocytes: an optimized four-color flow cytometry protocol for analysis of monocyte subsets.* J Cardiovasc Transl Res, 2011. **4**(2): p. 211-9.

97. Kawanaka, N., et al., *CD14+,CD16+ blood monocytes and joint inflammation in rheumatoid arthritis.* Arthritis Rheum, 2002. **46**(10): p. 2578-86.

98. Saleh, M.N., et al., *CD16+ monocytes in patients with cancer: spontaneous elevation and pharmacologic induction by recombinant human macrophage colony-stimulating factor.* Blood, 1995. **85**(10): p. 2910-7.

99. Sponaas, A.M., et al., *The proportion of CD16(+)CD14(dim) monocytes increases with tumor cell load in bone marrow of patients with multiple myeloma.* Immun Inflamm Dis, 2015. **3**(2): p. 94-102.

100. Chiu, Y.G., et al., *CD16 (FcRgammaIII) as a potential marker of osteoclast precursors in psoriatic arthritis.* Arthritis Res Ther, 2010. **12**(1): p. R14.

101. Lari, R., P.D. Kitchener, and J.A. Hamilton, *The proliferative human monocyte subpopulation contains osteoclast precursors.* Arthritis Res Ther, 2009. **11**(1): p. R23.

102. Faurschou, M. and N. Borregaard, *Neutrophil granules and secretory vesicles in inflammation.* Microbes Infect, 2003. **5**(14): p. 1317-27.

103. Poubelle, P.E., et al., *Differential expression of RANK, RANK-L, and osteoprotegerin by synovial fluid neutrophils from patients with rheumatoid arthritis and by healthy human blood neutrophils.* Arthritis Res Ther, 2007. **9**(2): p. R25.

104. Blimark, C., et al., *Multiple myeloma and infections: a population-based study on 9253 multiple myeloma patients.* Haematologica, 2014.

105. Silbermann, R. and G.D. Roodman, *Myeloma bone disease: Pathophysiology and management.* Journal of Bone Oncology, 2013. **2**(2): p. 59-69.

106. Hunt, N.C., et al., *Cellular mechanisms of bone resorption in breast carcinoma.* Br J Cancer, 2001. **85**(1): p. 78-84.

107. Shioya, M., et al., *Epithelial overexpression of interleukin-32alpha in inflammatory bowel disease.* Clin Exp Immunol, 2007. **149**(3): p. 480-6.

108. Pagliuca, F.W. and D.A. Melton, *How to make a functional beta-cell.* Development, 2013. **140**(12): p. 2472-83.

7.1 Website References

7.1.1 Figures

http://www.abcam.com/protocols/introduction-to-flow-cytometry

http://flowbook.denovosoftware.com/

7.1.2 Information

https://www.kreftregisteret.no/globalassets/cancer-in-norway/2011/cin2011_with_special_issue-nordcan_web.pdf

http://www.stemcell.com/en/Products/All-Products/EasySep-Human-CD138-Positive-Selection-Kit.aspx

http://www.bdbiosciences.com/us/applications/blood-collection/cell-biomarker-preservation/bd-vacutainerreg-cpttrade-mononuclear-cell-preparation-tube---sodium-heparin/p/362753

8 Appendices

Appendix I. Gating strategy and identification of granulocytes and monocytes in the bone marrow

(*A*)

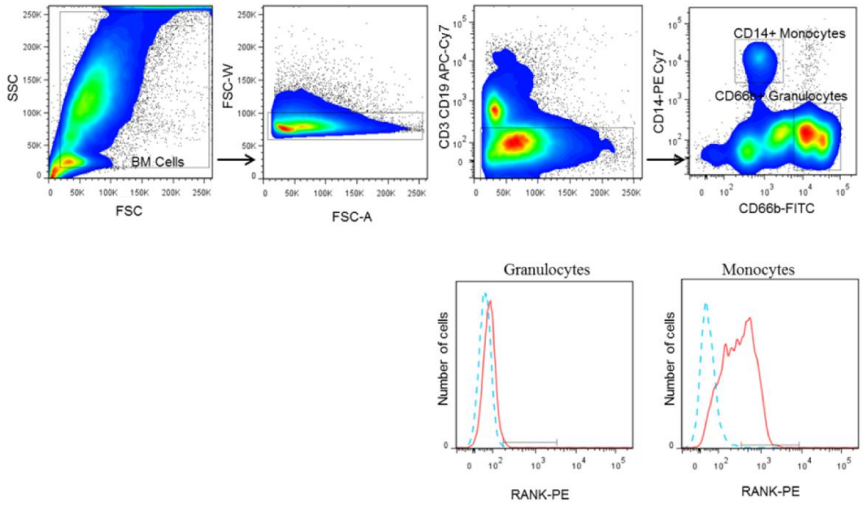

(*B*)

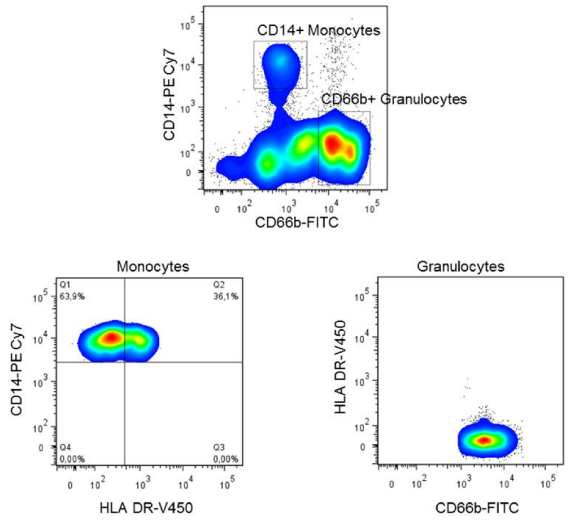

(A) Plots showing identification of monocytes and granulocytes in patient's bone marrow. Bone marrow cells were co-stained for RANK and a cocktail of antibodies against CD3, CD19, HLA DR, CD14 and CD66b. Monocytes and granulocytes were identified in the bone marrow and gates were set on live cells with FCS versus SSC, while doublets were excluded (FSC-A, FSC-W). Lineage cells ($CD3^+$, $CD19^+$) were further gated out and monocytes identified as $CD14^+$, $CD66b^-$ cells, and granulocytes as $CD66b^+$, $CD14^-$ cells. Dot plot of CD14 versus CD66b staining of a representative patient samples (*A*-upper left panel). Gated monocytes ($CD14^+$ $CD66b^-$) were HLA DR^+ and gated granulocytes ($CD66b^+$ $CD14^-$) were HLA DR^- (*B*- lower dot plots).

Appendix II. Gating strategy and identification of IL-32 expressing cells in myeloma cell lines and patient's bone marrow

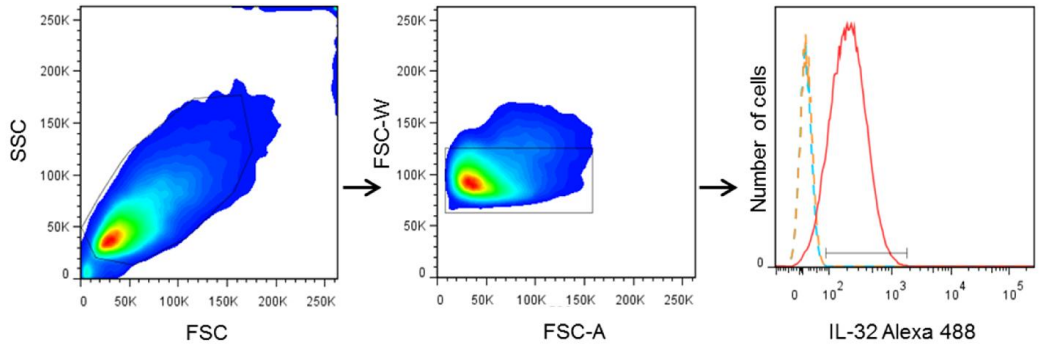

A representative example showing our gating strategy to identify IL-32 expressing cells in this study. Cells were fixed and subjected to intracellular staining with a goat anti IL-32 antibodies or isotype control, and then incubated with Alexa 488 conjugated anti-goat secondary antibodies or anti-goat Ig G Ab alone. Gates were set on live cells with FSC versus SSC and doublets were excluded (left and middle panel). Histogram showing IL-32 staining of the gated population (left panel). Isotype control and anti-goat Ig G antibodies were used as a negative control (blue and yellow dotted line respectively).

Appendix III. IL-32 expression in the myeloma bone marrow CD138$^+$ fraction

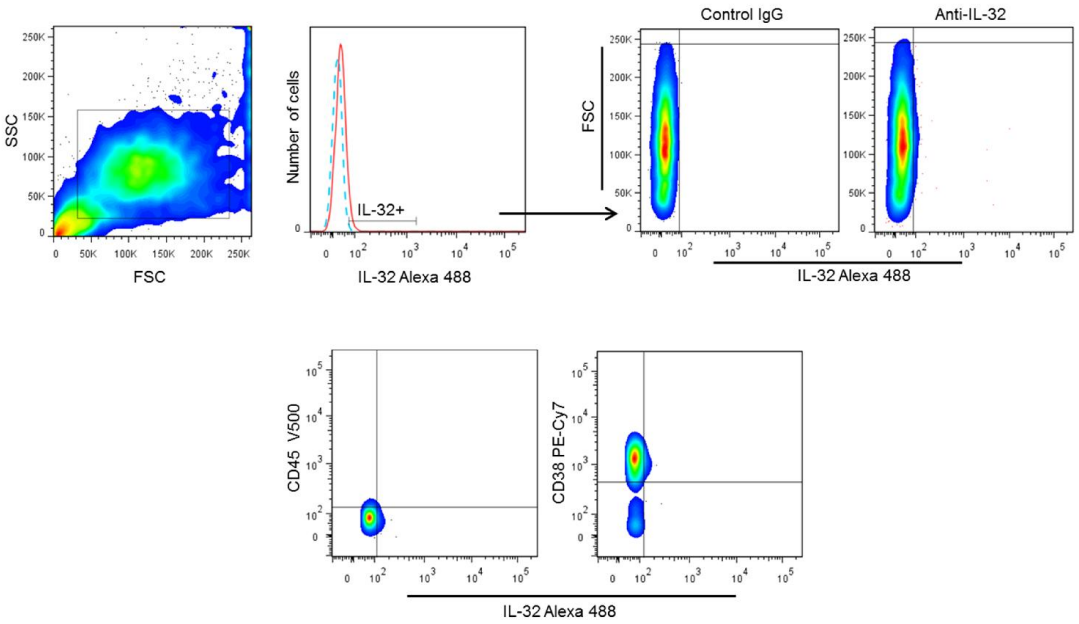

CD138$^+$ fraction was surface stained with antibodies against CD38 and CD45, fixed and then subjected to intracellular staining for IL-32 before analysis on LSR II Flow cytometer. The gate was set on live cells with FSC and SSC (upper right dot plot). Histogram is showing IL-32 staining of the gated population. The IL-32$^+$ population were checked for CD38 and CD45 expression (lower dot plots). The isotype control (dotted blue line) was used as a negative control to set the histogram and dot plot gates.

Appendix IV. IL-32 expression in the myeloma bone marrow CD138$^-$ fraction

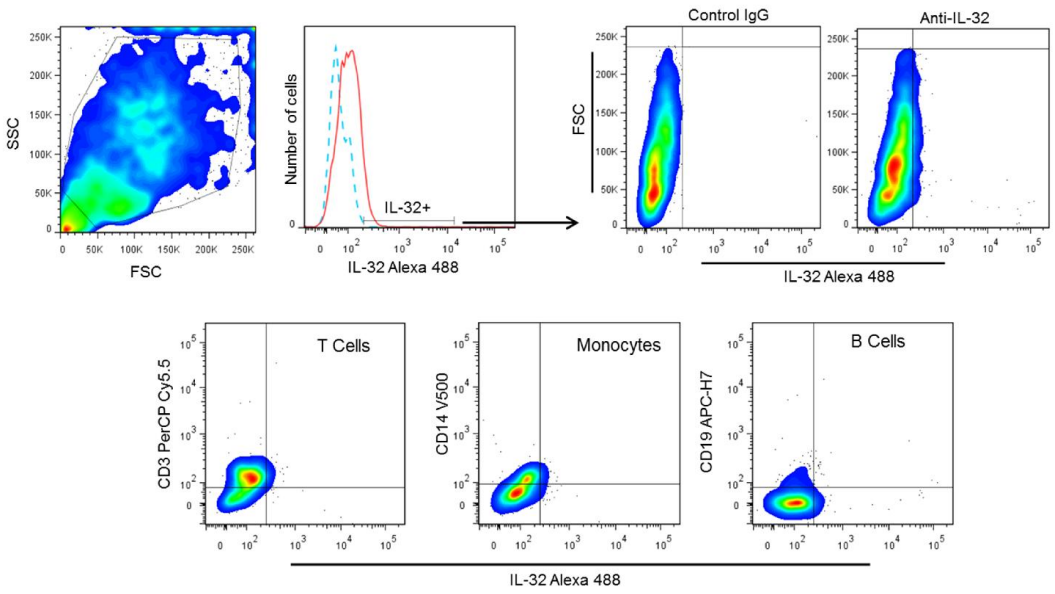

CD138$^-$ fraction was surface stained with antibodies against CD3, CD14, CD19, fixed and then subjected to intracellular staining for IL-32 before analysis on LSR II Flow cytometer. The gate was set on live cells with FSC and SSC (upper right dot plot). Histogram is showing IL-32 staining of the gated population. The IL-32$^+$ population was checked for CD3 (T cells), CD14 (monocytes) and CD9 (B cells) expression (lower dot plots). The isotype control (dotted blue line) was used as a negative control to set the histogram and dot plot gates.

Appendix V. Antibodies used for extra-cellular staining

Antibody-conjugate	Clone	Laser (nm)	Ex_{max} (nm)	Em_{max} (nm)	Filter Combination	Vendor	Catalog number
Anti- CD66b-FITC	G10F5	488	494	520	525/50	BD Pharmingen	555724
CD14-PE Cy7	M5E2	561	496	785	780/60	BD Pharmingen	561385
Anti- HLA-DR V450	L243	405	404	448	450/40	BD Pharmingen	655874
Anti- CD3-biotin	OKT3	-	-	-	-	eBioscience	13-0037
Anti-CD19-Biotin	HIB19	-	-	-	-	eBioscience	13-0199
Streptavidin APC-Cy7*		640	650	785	780/60	BD Pharmingen	554063
Anti-CD38 PE-Cy7	HIT2	561	496	785	780/60	BD Biosciences	335825
Anti-CD45 V500	HI30	405	415	500	525/50	BD Biosciences	655873
Anti-CD19 APC-H7	1D3	640	650	785	780/60	BD Biosciences	641395
Anti-CD14 BV 510	RPA-T8	405	405	510	525/50	Biolegend	301044
Anti-CD3 PerCP-Cy5.5	OKT3	488	482	695	695/40	eBioscience	45-003742
Anti-RANK PE	80704	561	496	578	575/26	R&D Systems	FAB683P

* Streptavidin APC-Cy7: Streptavidin not antibodies but a protein that has high affinity for biotin and here is conjugated with APC-Cy7.

Appendix VI. Antibodies used for intra-cellular staining

Antibody-conjugate	Clone	Laser (nm)	Ex_{max} (nm)	Em_{max} (nm)	Filter Combination	Vendor	Catalog number
Goat Anti-IL-32**	Cys2-Lys131	-	-	-	-	R&D Systems	AF3040
Normal Goat IgG		-	-	-	-	Santa Cruz	SC-3887
Anti-goat Alexa-488		488	495	519	530/30	Invitrogen	A1105

** Anti-IL-32 is un-conjugated goat anti-human polyclonal antibodies.

Appendix VII. List of reagents used for extra-cellular staining

Reagents	Vendor	Catalog number
Phosphate Buffered Saline (Ca^{++} and Mg^{++} free)	Thermo scientific	BR0014G
Bovine serum albumin	Sigma	Sigma A7030-50g
Human Fc Receptor binding inhibitor	eBioscience	14-9161
1-step Fix/Lyse Solution (10X)	eBioscience	00-5333-54

Appendix VIII. List of reagents used for intra-cellular staining

Reagents	Vendor	Catalog number
Phosphate Buffered Saline (Ca^{++} and Mg^{++} free)	Thermo scientific	BR0014G
Bovine serum albumin	Sigma	Sigma A7030-50g
Saponin (from quillaja bark)	Sigma	Sigma S7900
Paraformaldehyde	Alfa Aesar	30525-89-4